

Review

Potential Applications of Whisker Sensors in Marine Science and Engineering: A Review

Siyuan Wang ^{1,†} , Jianhua Liu ^{1,†}, Bo Liu ¹, Hao Wang ¹ , Jicang Si ¹, Peng Xu ^{2,*} and Minyi Xu ^{1,*} 

¹ Dalian Key Lab of Marine Micro/Nano Energy and Self-Powered Systems, Marine Engineering College, Dalian Maritime University, Dalian 116026, China; wsydlmu@dlmu.edu.cn (S.W.); ykliujianhua@163.com (J.L.); 1120220103@dlmu.edu.cn (B.L.); hao8901@dlmu.edu.cn (H.W.); sjc@dlmu.edu.cn (J.S.)

² Intelligent Biomimetic Design Lab, College of Engineering, Peking University, Beijing 100871, China

* Correspondence: pengxu@pku.edu.cn (P.X.); xuminyi@dlmu.edu.cn (M.X.)

† These authors contributed equally to this work.

Abstract: Perception plays a pivotal role in both biological and technological interactions with the environment. Recent advancements in whisker sensors, drawing inspiration from nature's tactile systems, have ushered in a new era of versatile and highly sensitive sensing technology. Whisker sensors, which mimic the tactile hairs of mammals, offer both high sensitivity and multifunctionality. They excel in capturing fine-grained environmental data, detecting various stimuli with precision, and finding applications in diverse domains. This review explores the integration of whisker sensors in potential marine applications. Categorized into six types, these sensors are invaluable for tasks such as marine structure monitoring, measurement instruments, tactile perception in marine robots, and non-contact sensing in the marine environment. Challenges and potential solutions are examined, along with the prospects of whisker sensors in the field of marine science and engineering. In an era that demands adaptable sensing solutions, whisker sensors emerge as pivotal components, enabling machines and devices to perceive and respond to external stimuli with heightened sensitivity and versatility. Their application in the marine domain holds substantial promise, propelling advancements in the realms of marine science and engineering.

Keywords: whisker sensors; tactile perception; marine science and engineering



Citation: Wang, S.; Liu, J.; Liu, B.; Wang, H.; Si, J.; Xu, P.; Xu, M. Potential Applications of Whisker Sensors in Marine Science and Engineering: A Review. *J. Mar. Sci. Eng.* **2023**, *11*, 2108. <https://doi.org/10.3390/jmse11112108>

Academic Editors: Rafael Morales and Christos Tsabaris

Received: 12 October 2023
Revised: 26 October 2023
Accepted: 2 November 2023
Published: 3 November 2023



Copyright: © 2023 by the authors. Licensee MDPI, Basel, Switzerland. This article is an open access article distributed under the terms and conditions of the Creative Commons Attribution (CC BY) license (<https://creativecommons.org/licenses/by/4.0/>).

1. Introduction

Perception forms the bedrock of both biological and machine interaction with the surrounding environment [1–6]. In the technological realm, the ability to perceive and respond to external stimuli remains a driving force behind ongoing innovations in sensor technology [7–10]. Optical and acoustic sensing technologies have consistently stood at the vanguard of this field, furnishing invaluable insights for our comprehension of the world surrounding us [11–14]. Nevertheless, there is a growing recognition of the need for more versatile and adaptable sensing solutions to meet the increasing demands of the modern world. Tactile sensing technology, serving as a pivotal complement to conventional optical and acoustic sensing technologies, has equipped machines and devices with broader sensing and responsive capabilities. Research and applications in this sphere have achieved significant breakthroughs across multiple domains [15–20]. A current trend in tactile sensing technology involves a growing inclination towards biomimicry, where researchers draw inspiration from nature's own sensory systems to create sensors capable of emulating the complexity and adaptability found in living organisms. This bio-inspired approach to tactile sensing has given rise to a gamut of biomimetic tactile sensors, each replete with unique advantages and applications [21–24].

Among the myriad biomimetic tactile sensors that have attracted considerable attention, whisker sensors stand out as a distinctive and promising category due to their

exceptional ability to discern critical environmental cues [25–28]. They derive inspiration from the tactile sensing capabilities displayed by various animals, particularly mammals. Whiskers are highly sensitive elongated tactile hairs, and these remarkable appendages play an indispensable role in detecting and interpreting the surrounding environment, endowing animals with vital information about objects, surfaces, and even fluid dynamics [29–34]. Since the conceptualization of whisker sensors in 1987 [35], researchers worldwide have conducted extensive investigations into whisker sensors based on various sensing principles, yielding numerous exciting research outcomes. Compared to conventional tactile sensors, whisker sensors offer several advantages, with their most prominent attribute being high sensitivity, an inherent characteristic of their biomimetic design. Whisker sensors excel in capturing fine-grained environmental data, providing a more comprehensive understanding of the surroundings than traditional tactile sensors [36,37]. Traditional tactile sensors often struggle to discern subtle changes in touch, pressure, or texture, while whisker sensors, with their flexible and responsive whisker-like structures, can minutely discriminate variations in the environment [38–41]. This heightened sensitivity renders them exceptionally valuable in applications where precision and accuracy stand as paramount requisites. Additionally, whisker sensors exhibit significant versatility and are capable of detecting various stimuli, including static and dynamic touches [42–44], airflow [45,46], vibrations [47,48], and even fluid flow [49,50]. The multifunctionality of whisker sensors expands their applicability across various fields, including robotics, automation, environmental monitoring, and scientific research.

While the number of existing applications remains limited, the field of marine science and engineering consistently emerges as one of the most promising arenas for whisker sensors, often denoted as ‘marine whisker sensors’. Marine whisker sensors could find diverse applications both underwater and at the sea surface. In underwater applications, these sensors can seamlessly integrate into robotic systems, particularly remotely operated vehicles (ROVs), extending the realm of touch to achieve precise navigation in intricate underwater terrains while adeptly detecting obstacles and mapping underwater topography [51,52]. In nearshore applications, these sensors can be deployed on offshore drilling platforms and nearshore structures, assisting in the detection of corrosion, cracks, or anomalies in critical infrastructure components such as pipelines, tanks, and support structures [53,54]. Whisker sensors installed on inspection robots can meticulously scrutinize ship hulls and interiors, promptly identifying corrosion, leaks, or structural damage, thereby enhancing the safety and durability of maritime vessels [55,56]. Furthermore, these sensors play a pivotal role in ocean pipeline monitoring, astutely detecting leaks, dents, and external hazards, ensuring the uninterrupted operation of underwater pipelines [57,58]. In addition to safeguarding infrastructure, whisker sensors can also assume a crucial role in the navigation and collision avoidance of ships and underwater vehicles, leveraging their real-time close-range sensing capabilities to prevent accidents and minimize damage [27,59]. On the water’s surface, whisker sensors can serve as oceanographic instruments, accumulating a wealth of environmental information [60,61]. Figure 1 illustrates several accomplishments of marine whisker sensors within four primary application scenarios. Whisker sensors, due to their precision and real-time data acquisition capabilities, offer a versatile solution for applications both underwater and on the sea surface. This contribution serves to advance the fields of marine science and engineering.



Figure 1. Potential applications of whisker sensors in marine science and engineering. Reproduced with permission. Ref. [62] Copyright 2018, IOP Publishing. Reproduced with permission. Ref. [63] Copyright 2021, MDPI. Reproduced with permission. Ref. [61] Copyright 2012, IOP Publishing. Reproduced with permission. Ref. [64] Copyright 2017, Elsevier B.V. Reproduced with permission. Ref. [65] Copyright 2021, AAAS. Reproduced with permission. Ref. [66] Copyright 2022, Elsevier B.V. Reproduced with permission. Ref. [67] Copyright 2022, Elsevier B.V. Reproduced with permission. Ref. [68] Copyright 2023, WILEY-VCH.

This review endeavors to explore the intricacies of whisker sensors and their integration into marine applications. In the subsequent sections, we will scrutinize the fundamental distinctions in whisker sensor technology and expound upon its potential applications in marine science and engineering. To commence, we will undertake a comprehensive examination of the typical categories of whisker sensors, categorizing them into six primary types: optical whisker sensors, magnetic whisker sensors, resistive whisker sensors, capacitive whisker sensors, piezoelectric whisker sensors, and triboelectric whisker sensors. We will follow this taxonomy to systematically introduce the current state of marine whisker sensors, presenting their potential applications in four key domains: marine structure monitoring, marine measurement instruments, tactile perception in marine robots, and non-contact sensing in the marine environment. This endeavor will illuminate the extensive potential that these sensors hold within the realm of marine science and engineering. Lastly, we will enumerate the challenges currently confronting marine whisker sensors and explore potential remedies. In addition, we will conduct a comprehensive analysis of

the prospects associated with marine whisker sensors, with the intention of emphasizing their significance in diverse contexts and the exciting opportunities they offer for the future of marine science and engineering.

2. Typical Categories of Whisker Sensors

The whisker sensor represents a significant advancement in tactile sensing technology, drawing inspiration from the remarkable perceptual abilities observed in biological organisms. Its fundamental operation revolves around detecting strain variations within whiskers when exposed to external stimuli. This section presents a comprehensive review of whisker sensors, classifying them into six primary categories based on their underlying sensing principles: optical whisker sensors, magnetic whisker sensors, resistive whisker sensors, piezoelectric whisker sensors, capacitive whisker sensors, and triboelectric whisker sensors.

2.1. Optical Whisker Sensors

Optical sensing technology, as one of the most widely employed sensing methodologies in contemporary applications, has witnessed significant advancements in the maturity of its sensing components [69–71]. The construction of whisker sensors utilizing optical sensing elements presents a direct and viable approach. Depending on the optical sensing mechanism employed, optical whisker sensors can assume diverse configurations. For instance, in the research conducted by Wang et al., whisker sensors were meticulously designed and produced using optical polymer-formed whiskers [72], as visually represented in Figure 2A. These whiskers, emerging from the central core of a seven-core optical fiber (SCF), connect to solid pendulums, thereby forming six parallel Fabry–Pérot interferometers between the SCFs. The fundamental sensing principle of this configuration is delineated in Figure 2B, where it relies on multi-beam interference phenomena. When subjected to external stimuli causing deformation in the optical polymer whiskers, the ensuing alterations in cavity length are translated into variations in interference signals. Figure 2C depicts an experimental setup for this sensor where solid pendulums induce deformation in the optical polymer whiskers and sensory data are acquired using an imaging system.

Figure 2D presents an alternative design in which whiskers, equipped with magnets at their bases, are affixed to an elastomeric membrane housing numerous tracking points [73]. The changes in position of both the whisker bases and tracking points are captured by a camera and subsequently analyzed through target tracking algorithms to extract feature data. Figure 2E showcases typical images of whisker deflections along the z-axis, with the experimental arrangement detailed in Figure 2F. A similar design is illustrated in Figure 2G, albeit with a greater number of whiskers constituting a sensing array to augment sensing capabilities [74]. These 3D-printed whiskers are affixed to a flexible base and further connected to an image-capturing module relying on cameras. Spot tracking algorithms are harnessed to monitor changes in the positions of the pins, facilitating the extraction of sensory information. Physical representations of this whisker array sensor are portrayed in Figure 2H. It is imperative to acknowledge that while the approach of using cameras to identify and track points for detecting whisker deformation is conceptually simpler in design, it is confined to capturing two-dimensional motion states, thereby exhibiting limitations in sensing dimensions. Conversely, the utilization of optical polymer whiskers for sensing offers higher-dimensional sensing capabilities but necessitates more intricate system designs, posing challenges in the miniaturization of the entire whisker sensing system. Another crucial consideration lies in the fact that fiber-optic-based whisker sensors offer greater potential for achieving high precision levels in sensing capabilities. The pursuit of integrating and miniaturizing data acquisition devices may indeed represent a pivotal research direction for enhancing the application potential of optical whisker sensors.

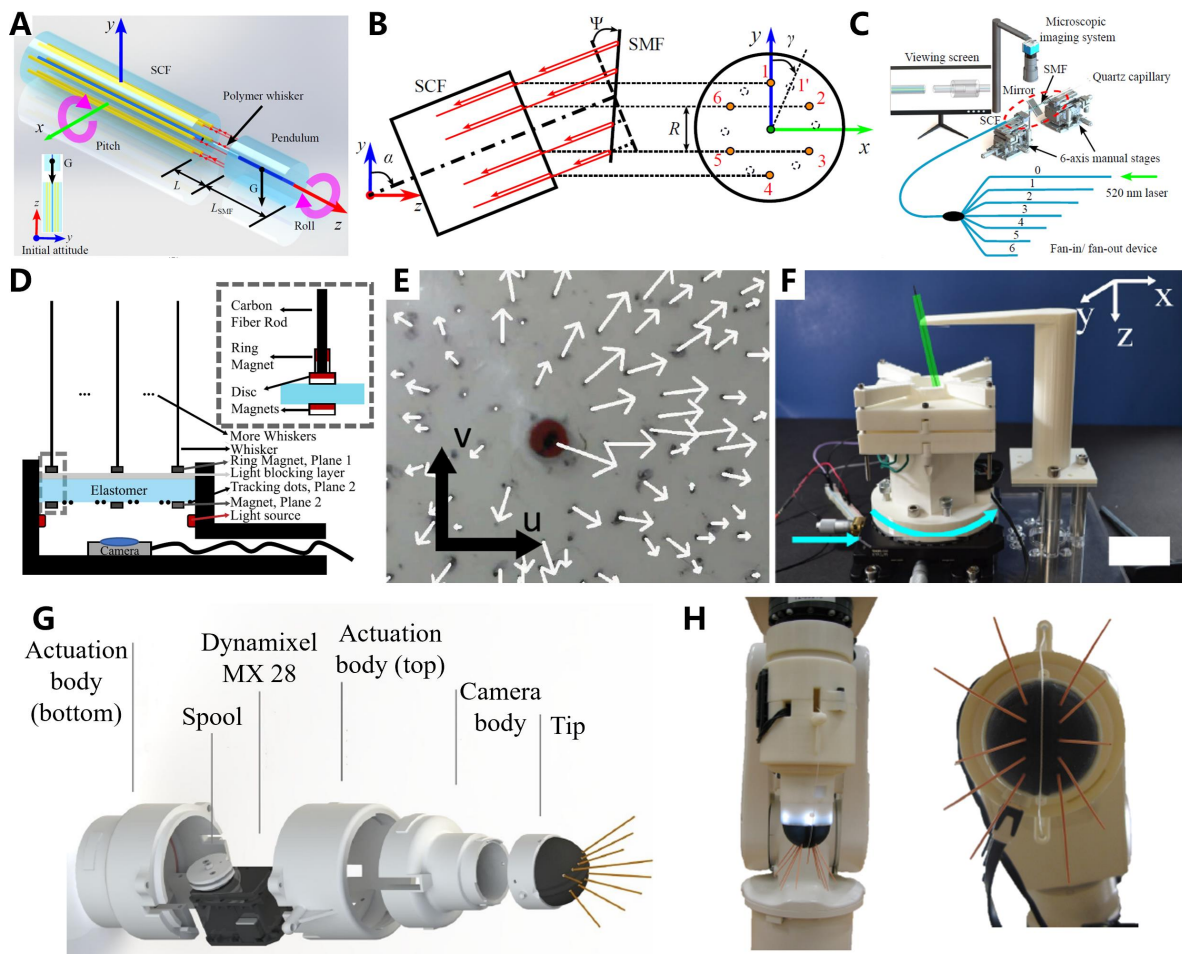


Figure 2. Optical whisker sensors. (A). Schematic diagram of the whisker-inspired fiber attitude sensor. (B). Schematic diagram of working principle of the whisker-inspired fiber attitude sensor. (C). The schematic diagram of the experimental setup. (A–C) Reproduced with permission. Ref. [72] Copyright 2023, IEEE. (D). Schematic diagram of the WhiskSight sensor. (E). The motion of a tracker dot on the whisker magnet or the elastomer. (F). The schematic diagram of the experimental setup. (D–F) Reproduced with permission. Ref. [73] Copyright 2021, IEEE. (G). Schematic diagram of the design of the dynamic TacWhisker array. (H). Physical picture of TacWhisker array. (G,H) Reproduced with permission. Ref. [74] Copyright 2018, IEEE.

2.2. Magnetic Whisker Sensors

Magnetic whisker sensors represent one of the predominant categories of whisker sensors currently employed, primarily relying on the incorporation of Hall sensors in their design [75–78]. Owing to the compact dimensions, multi-dimensional capabilities, and robust environmental adaptability inherent in Hall sensors, magnetic whisker sensors can be developed with enhanced miniaturization and integration. Figure 3A elucidates the conceptual framework of a typical magnetic whisker sensor, featuring a whisker structure affixed to a base via a spring mechanism, with the whisker’s base housing a permanent magnet [79]. Variations in the position of the whisker’s base are registered by an underlying Hall effect sensor. This mechanical configuration can be simplified to a fundamental torsion spring model, as demonstrated in Figure 3B, allowing for the modulation of the whisker’s sensitivity to external stimuli through adjustments to the spring’s elasticity coefficient. Figure 3C provides a visual representation of this sensor. Leveraging the versatile attributes of Hall sensors, magnetic whisker sensors are not confined to conventional design paradigms.

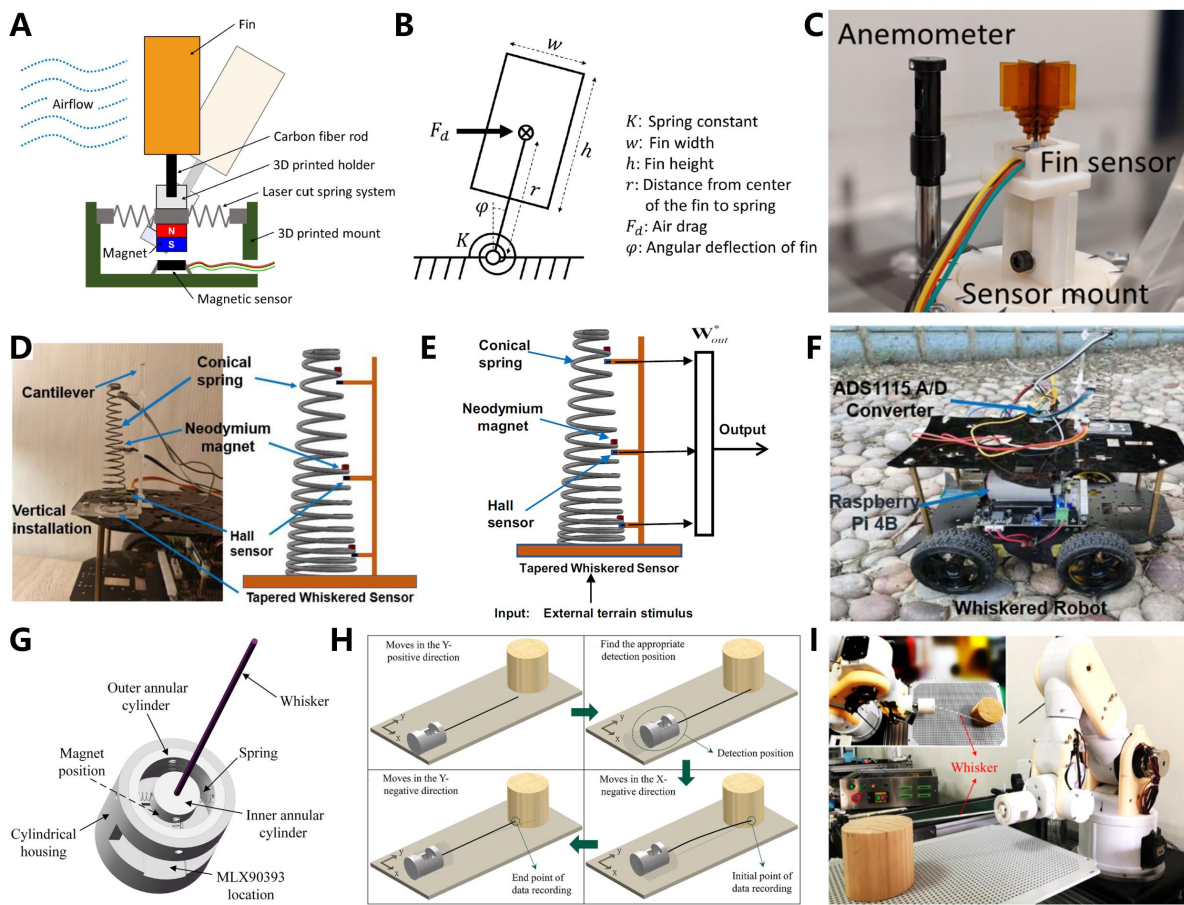


Figure 3. Magnetic whisker sensors. (A). Schematic diagram of the fin sensor. (B). Torsional spring model of the airflow sensing system with modeling parameters. (C). Physical picture of the fin sensor. (A–C) Reproduced with permission. Ref. [79] Copyright 2020, IEEE. (D). Schematic diagram of the tapered whisker sensor and model. (E). Schematic diagram of the tapered whisker-based reservoir computing system. (F). A differential-drive mobile robot with a bio-inspired tapered whisker sensor. (D–F) Reproduced with permission. Ref. [80] Copyright 2023, Springer Nature. (G). Schematic diagram of the structure of whisker sensor. (H). Schematic diagram of sensor scanning object. (I). Physical picture of the experimental device. (G–I) Reproduced with permission. Ref. [81] Copyright 2022, IOP Publishing.

Figure 3D introduces an alternative configuration—a conical magnetic whisker sensor composed of high-carbon material springs, three permanent magnets, and corresponding linear Hall sensors [80]. This conical whisker sensor serves the purpose of discerning diverse terrains encountered during robotic locomotion. The forces imparted during the robot’s movement are translated into spring deformations, and the data feature matrix collected by the Hall sensor can undergo further analysis via machine learning techniques, as depicted in Figure 3E. Figure 3F offers a tangible depiction of a robot navigation system constructed around this sensor, accentuating the advantage of the heightened integration facilitated by magnetic whisker sensors. Processing and analysis of sensory data can be efficiently executed using a single microcontroller, enabling the realization of intended functionalities. Figure 3G presents a whisker sensor predicated on three-axis Hall sensors and characterized by a straightforward cylindrical structure [81]. This sensor excels in perceiving the external contours of objects through tactile means, as exemplified in Figure 3H. By maneuvering the whiskers across the surface of the target object within a two-dimensional plane, it emulates the sensory mechanism akin to the tactile perception employed by select biological organisms equipped with sensory whiskers. Figure 3I offers a tangible representation of this sensor alongside its application scenario. When integrated

into a robotic arm, the whisker sensor adeptly discerns the surface contours of objects. However, it is crucial to acknowledge the vulnerability of Hall sensors to temperature fluctuations, rendering them ineffective in certain practical contexts. Furthermore, the elevated cost associated with Hall sensors poses a hindrance to the widespread adoption of magnetic whisker sensors.

2.3. Resistive Whisker Sensors

Resistive whisker sensors constitute a category of sensors that employ resistive materials to enable sensory functions. Their sensing principle is rooted in the resistive effect, wherein the detection of whisker deformation relies on measuring changes in the resistance of the resistive material in response to external stimuli. These sensors are known for their structural simplicity, low energy consumption, and wide detection range. This design approach provides a plethora of material choices, including silicon [82,83], carbon [84,85], graphene [86,87], and more [88]. Figure 4A depicts a paper-based whisker sensor utilizing graphite material. Its sensing mechanism originates from micro-contact changes within the graphite layers [89]. When the whisker experiences strain due to external stimuli, the overlaid graphite layers may detach, resulting in significant resistance changes. Figure 4B presents its output performance, revealing markedly opposing outputs in response to strains in two different directions, thereby demonstrating a well-defined pattern. Figure 4C introduces a three-dimensional strain whisker sensor based on carbon nanotubes [90]. This sensor employs a self-assembly technique to deposit modified single-walled carbon nanotubes onto a sensor body composed of polydimethylsiloxane (PDMS), forming a stretchable conductive film for strain measurement. The manufactured three-dimensional strain whisker sensor is depicted in Figure 4D, exhibiting millimeter-level precision. This whisker sensor can also be utilized to construct a strain sensing array, as exemplified in Figure 4E. The entire fabrication process relies solely on 3D printing technology and material processing techniques. The performance of resistive whisker sensors can be further enhanced through advanced processing of resistive materials.

As illustrated in Figure 4F, Takei et al. proposed a whisker sensor based on a highly adjustable composite film comprising carbon nanotubes and silver nanoparticles [91]. Its resistance displays exceptional sensitivity to strain, reaching up to 8% per Pascal. Figure 4G delineates the circuitry configuration of the sensor's top and bottom, with the top electrode exhibiting significantly higher resistance than the bottom electrode. Consequently, changes in resistance solely impact the sensor's output through the top electrode, thereby facilitating extensive resistance adjustability. By arranging seven whisker sensors into a hemispherical array, the sensory system can discern fluid flow, as demonstrated in Figure 4H. Notably, despite achieving a higher degree of miniaturization, resistive whisker sensors are still constrained by their reliance on external current supply for data acquisition, which impedes further integration and miniaturization. Additionally, they exhibit notable nonlinearity and weak output signals in high-strain scenarios, thereby retaining inherent limitations.

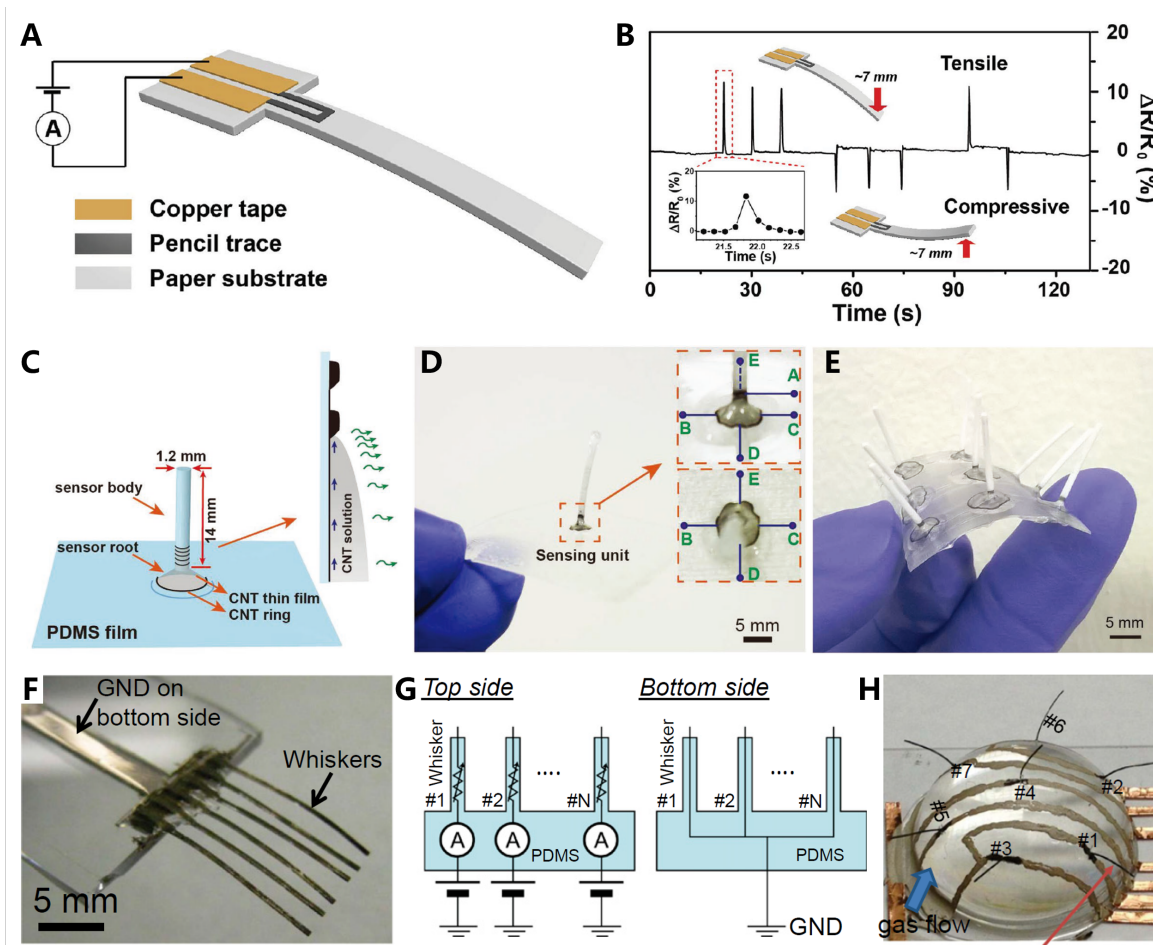


Figure 4. Resistive whisker sensors. (A). Schematic diagram of the pencil-drawn e-whisker device. (B). Schematic diagram of the response performances of the pencil-drawn e-whisker. (A,B) Reproduced with permission. Ref. [89] Copyright 2016, WILEY-VCH. (C). Schematic diagram of the 3D-structured stretchable strain sensors with out-of-plane multirings. (D). Physical picture of a fabricated 3D-structured stretchable strain sensor. (E). Physical picture of the 3D-structured stretchable strain sensor array. (C–E) Reproduced with permission. Ref. [90] Copyright 2018, WILEY-VCH. (F). Physical picture of a fully fabricated e-whisker array. (G). Schematic diagram of the circuit of the e-whiskers. (H). Physical picture of an array of seven vertically placed e-whiskers. (F–H) Reproduced with permission. Ref. [91] Copyright 2014, National Academy of Science.

2.4. Capacitive Whisker Sensors

Capacitive whisker sensors employ various types of capacitors as sensing elements [92–94]. External stimuli cause strain on the whisker, resulting in a change in the relative position between the two plates of the capacitor, leading to a modification in capacitance. Detecting this change in capacitance provides strain information. These sensors offer several advantages, including high sensitivity, low energy consumption, and insensitivity to temperature variations. Figure 5A illustrates a typical design of a capacitive whisker sensor based on the basic principle of a parallel-plate capacitor [95]. This sensor comprises two cones with metal-coated surfaces facing each other, sealed with conductive silver epoxy resin for waterproofing. Insulating silicone oil fills the space between the capacitor plates to provide a sufficient dielectric constant. The inner cone, housing the whisker, is affixed to the outer cone using PDMS, offering both sealing and appropriate damping and restoring forces. While the nested cone structure prevents the capacitor plates from being perfectly parallel, it increases the surface area of the plates, enhancing the signal output amplitude. Figure 5B presents a physical representation of the sensor. In comparison to prior work

by this research team, this version of the sensor employs gold-plated silver epoxy resin capacitor plates to mitigate corrosion. It eliminates a separate waterproof layer that used to cover the plates, reducing parasitic capacitance in series with the gap between the plates and significantly improving signal strength. Furthermore, shielded wires are employed to minimize electromagnetic noise.

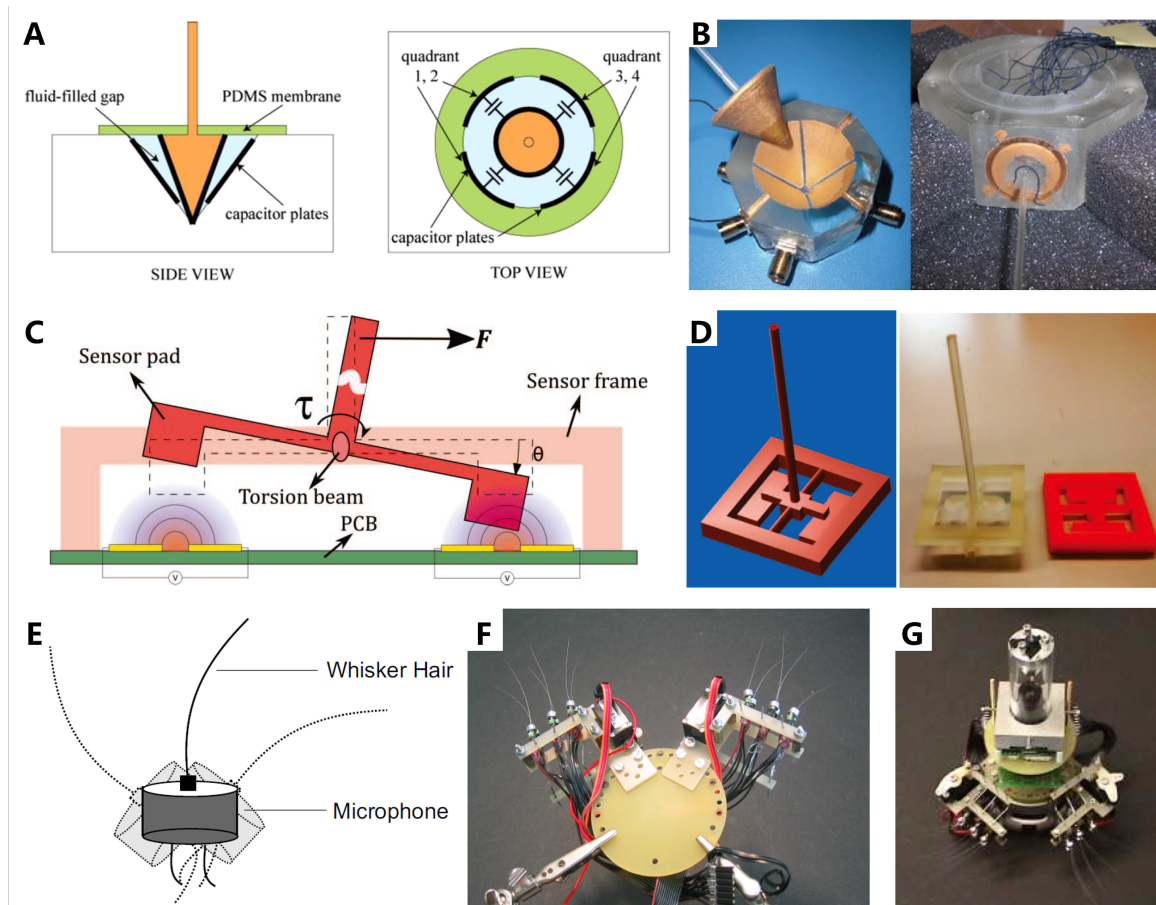


Figure 5. Capacitive whisker sensors. (A). Schematic diagram of the basic cone-in-cone sensor design. (B). Physical picture of the cone-in-cone sensor with gold plating and no explicit waterproofing layer over the capacitor plates. (A,B) Reproduced with permission. Ref. [95] Copyright 2016, IOP Publishing. (C). Schematic diagram of the capacitive sensing using dielectrics driven into co-planar capacitors. (D). Physical picture of the 3D CAD design of whisker sensor and printed whisker sensor. (C,D) Reproduced with permission. Ref. [96] Copyright 2016, IEEE. (E). Schematic diagram of the movement of the whisker on the microphone. (F). Physical picture of the layer containing the two whisker arrays. (G). Physical picture of the AMouse with its whiskers and the omnidirectional camera. (E–G) Reproduced with permission. Ref. [97] Copyright 2014, Citeseer.

Figure 5C presents a sensing mechanism for a whisker sensor based on a coplanar capacitance design [96]. Placing the whisker model on a patterned printed circuit board (PCB) allows the measurement of changes in coplanar capacitance on the PCB to determine the force and torque at the base of the whisker. The physical representation is shown in Figure 5D. The whisker is entirely 3D-printed, with the base made of polylactic acid (PLA) and the whisker part made of transparent resin. The base can be modeled as a torsion spring, and sensitivity is effectively improved by optimizing electrode patterns and reducing the stiffness of the torsion spring. Figure 5E proposes a more integrated solution where the whisker is directly attached to a capacitive microphone [97]. The microphone sensor offers a good signal-to-noise ratio and can track higher-frequency whisker movements but cannot provide information about the direction of whisker deflection, which is a limitation of

microphone-based sensors. Figure 5F displays an image containing two whisker sensor arrays. Whiskers can be fixed at multiple positions to achieve different sensing modes. This sensing array can be integrated into robots, as demonstrated in Figure 5G, to augment tactile perception dimensions. Together with additional optical and acoustic sensors, it forms the robot's perception system, enabling effective navigation. It should be noted that capacitive sensors commonly suffer from parasitic capacitance, electromagnetic interference, and crosstalk between array elements, which can affect their performance. This lack of stability has limited in-depth research on this principle in the field of whisker sensors.

2.5. Piezoelectric Whisker Sensors

Piezoelectric whisker sensors are a specialized category of sensors designed to detect whisker strain by harnessing the piezoelectric effect inherent in certain materials when subjected to external stimuli. In essence, these sensors leverage the piezoelectric effect. This effect entails the polarization of internal charges within the piezoelectric material, resulting in the generation of charges on the material's surface. A distinctive feature of piezoelectric whisker sensors is their self-driving capability, allowing them to function effectively without the need for an external energy supply. This characteristic proves particularly advantageous in energy-constrained scenarios, such as robotics [98–100]. The schematic structure of a piezoelectric whisker sensor based on polyvinylidene difluoride (PVDF) for flow sensing is depicted in Figure 6A [101]. PVDF is affixed to a metal core, its surface coated with a conductive silver layer serving as electrodes. The polarization process renders the metal core the negative electrode, while the conductive silver layer becomes the positive electrode. A flexible optical fiber, approximately 300 μm in diameter, replaces the metal core, and waterproof adhesive is applied to ensure water resistance. During polarization, the electric field direction follows a radial path along the optical fiber, resulting in radial polarization, as shown in Figure 6B. The physical representation of this sensor and the experimental setup are presented in Figure 6C.

The sensing mechanism of another piezoelectric whisker sensor, based on lead zirconium titanate (PZT) material [102], is illustrated in Figure 6D. When exposed to fluid loads, the interaction between the sphere head and the fluid impacts the mechanical response of the sphere, inducing the piezoelectric effect. Coupled mechanical response electric signals can then be collected to analyze the whisker's strain. As depicted in Figure 6E, this sensor comprises PZT dual piezoelectric chips, a steel whisker, and a glass sphere tip. The sphere head enhances interaction with the fluid, reduces the operating frequency, and aids in interpreting fluid loads. The physical representation of the sensor is shown in Figure 6F. Due to their uncomplicated structure and self-driving attributes, piezoelectric whisker sensors can be fabricated on a microscale [103], as illustrated in Figure 6G. This sensor is produced using electrohydrodynamic jet printing technology, with a whisker sensor diameter of only 120 μm and a well-defined linear output pattern. Figure 6H elucidates the structural components and sensing mechanism of the sensor. Cantilevered piezoelectric sensors are affixed to a PCB, and the whisker and electrode layers are connected to the PCB using silver paste to secure the sensor and extract signals. When the whisker undergoes bending deformation due to external loads, the polarization surface of the piezoelectric ceramic generates alternating voltage signals due to mutual stretching and compression deformation. Figure 6I displays the microstructure of the whisker. However, addressing the low-level output signals of piezoelectric whisker sensors often requires the use of high-input impedance circuits or charge amplifiers. Additionally, due to the inherent characteristics of piezoelectric materials, challenges involving poor low-frequency performance and maintenance difficulties need to be addressed in future research.

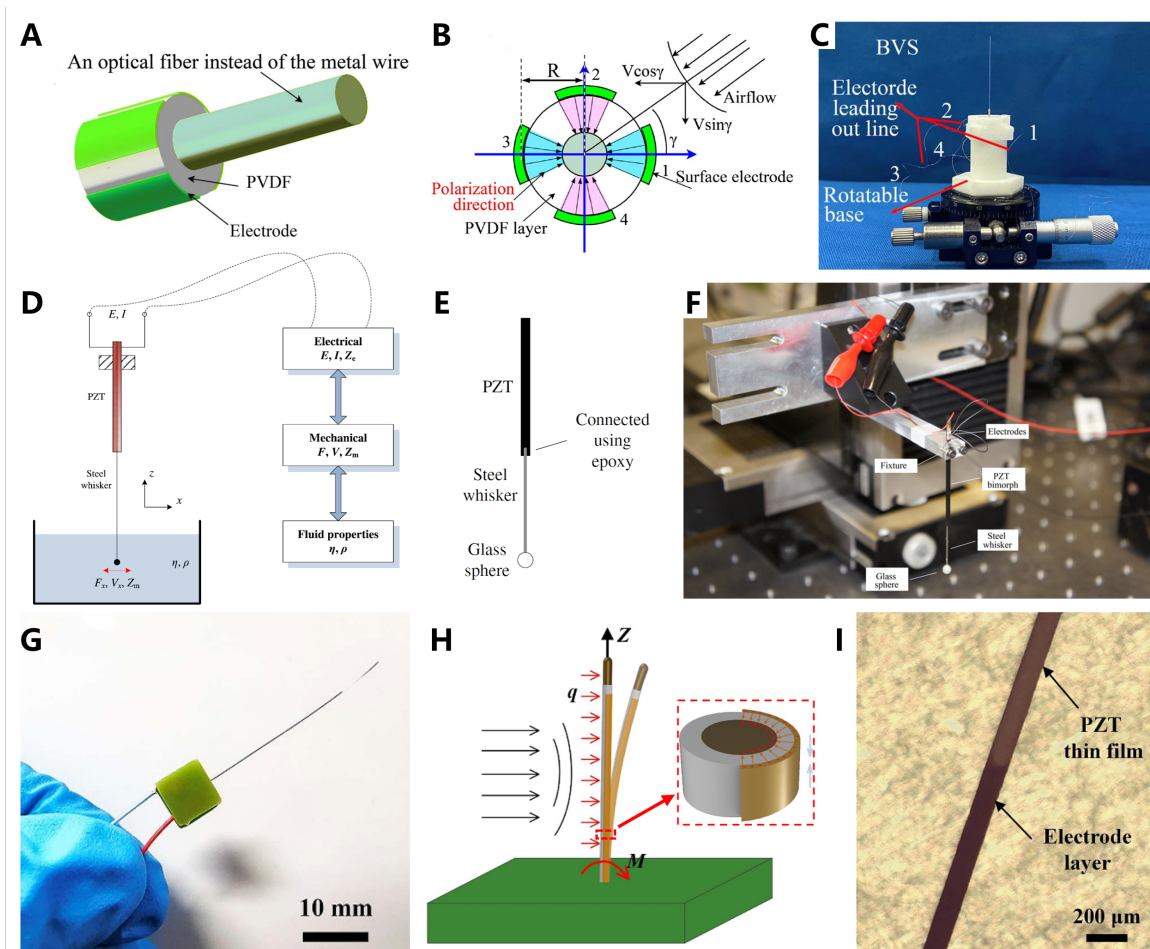


Figure 6. Piezoelectric whisker sensors. (A). Schematic diagram of the bionic whisker sensor based on PVDF fiber. (B). Schematic diagram of the cross-section of the bionic whisker sensor. (C). Physical picture of the bionic whisker sensor. (A–C) Reproduced with permission. Ref. [101] Copyright 2022, IEEE. (D). Schematic diagram of the whisker transducer and its working principle. (E). Schematic diagram of the connection of components. (F). Physical picture of the whisker transducer. (D–F) Reproduced with permission. Ref. [102] Copyright 2013, IOP Publishing. (G). Physical picture of the fabricated sensor. (H). Schematic diagram of the working principle of high-aspect-ratio cantilevered sensing element. (I). Physical picture of the PZT thin film surface of the cantilever-type piezoelectric transducer. (G–I) Reproduced with permission. Ref. [103] Copyright 2023, IOP Publishing.

2.6. Triboelectric Whisker Sensors

Triboelectric whisker sensors utilize the triboelectric effect and electrostatic induction to convert the minute mechanical energy generated by whisker strain into electrical signals, facilitating the analysis of strain information in whiskers. In comparison to piezoelectric sensors, triboelectric sensors possess the advantages of self-driving capabilities, higher output voltage, and lower cost, rendering them more advantageous in the development of sensing systems [104–106]. Figure 7A illustrates the structural composition of a triboelectric whisker sensor based on a membrane-structured triboelectric nanogenerator (TENG) [107]. The artificial whisker is composed of silicone gel, with its base situated in the center of the TENG sensing unit. The TENG sensing unit employs acrylic as the substrate with copper deposition on the surface serving as the electrode layer. The upper substrate incorporates polytetrafluoroethylene (PTFE) film with copper deposition on one side, functioning as the dielectric layer and another electrode layer. The sensing principle of the TENG relies on the coupling effect between the triboelectric effect and electrostatic induction, as depicted in Figure 7B. When the whisker undergoes strain, it initiates contact and separation between

the dielectric layer and electrode layers of the TENG, akin to two parallel capacitors. With increasing strain, the left part of the PTFE contacts the Cu electrode, undergoing charge neutralization, resulting in the TENG's output contribution solely from the right part in this model.

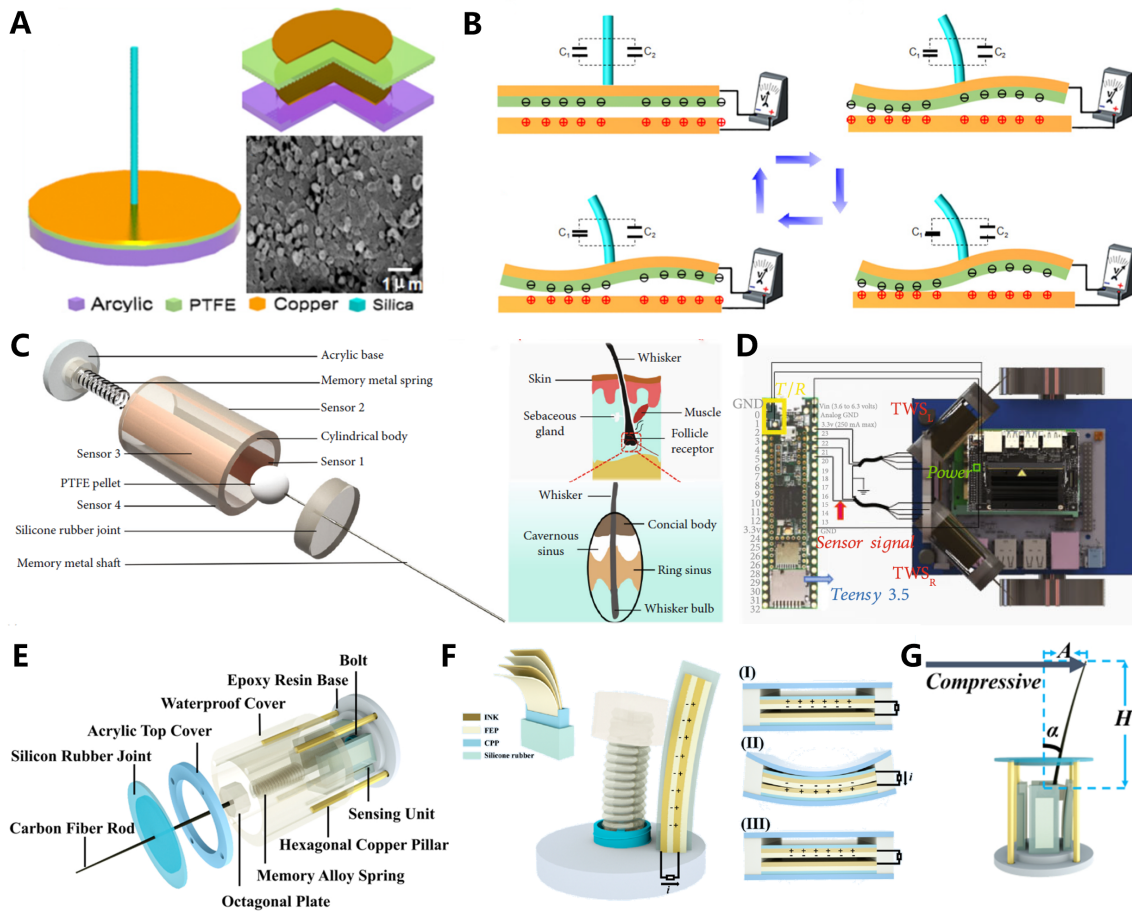


Figure 7. Triboelectric whisker sensors. (A). Schematic diagram of the structural design of the triboelectric whisker sensor. (B). Schematic diagram of a full cycle of the electricity generation process of the triboelectric whisker sensor. (A,B) Reproduced with permission. Ref. [107] Copyright 2015, IOP Publishing. (C). Schematic diagram of the basic structure of the bionic follicle whisker sensor. (D). Schematic diagram of the electronic module used for potential application demonstrations. (C,D) Reproduced with permission. Ref. [65] Copyright 2021, AAAS. (E). Schematic diagram of the structural design of the bionic whisker sensor. (F). Schematic diagram of the structure diagram, force diagram, and power generation of the sensing unit. (G). Schematic diagram of the bionic whisker sensor state under external load. (E–G) Reproduced with permission. Ref. [67] Copyright 2022, Elsevier B.V.

Another advantageous feature of TENG is its high flexibility, enabling the design of diverse structures employing various materials. One such example is a follicle-inspired triboelectric whisker sensor closely mimicking the follicle structure of a mouse whisker [65], as exemplified in Figure 7C. This structure comprises a soft silicone rubber junction (Ecoflex 00-20), a 3D-printed cylindrical shell (polylactic acid), and a rigid 3D-printed base. The base incorporates a spring connected to a PTFE sphere, serving as the dielectric layer, with the spring providing ample damping and restoring force. The artificial whisker is constructed from shape memory alloy, and the inner surface of the shell symmetrically hosts four copper films as electrode layers. Due to the high output voltage characteristics of TENGs, this sensor can be directly integrated with robots without the need for additional circuits,

as demonstrated in Figure 7D. Moreover, through the utilization of a sealed structure and waterproof materials, triboelectric whisker sensors exhibit significant potential for applications in underwater environments. Figure 7E showcases a biomimetic triboelectric whisker sensor inspired by sea otter whiskers [67]. Its structure primarily includes a sealed housing, carbon fiber artificial whiskers, and four TENG sensing units. Figure 7F details the structure and generation mechanism of the TENG sensing unit. The sensing unit employs fluorinated ethylene propylene (FEP) film as the dielectric layer, conductive ink as the electrode layer, and is coated with a layer of cast polypropylene (CPP) film for electrostatic shielding. The external layer is enveloped in silicone to ensure waterproofing. When the whisker experiences strain, the internal sensing unit undergoes force, bringing the dielectric materials into contact, leading to charge transfer during the contact-separation process, thereby generating electrical signal outputs. A more intuitive sensing process is depicted in Figure 7G. It is noteworthy that triboelectric whisker sensors are typically suited for measuring dynamic force changes and may exhibit enhanced sensing capabilities in specific application scenarios.

3. Potential Applications of Whisker Sensors in Marine Science and Engineering

Whisker sensors have emerged as a distinct category within the realm of tactile sensors, offering innovative solutions to address tactile perception challenges. Leveraging their diverse principles and structural adaptability, whisker sensors find significant utility in marine potential applications; these can be referred to as marine whisker sensors. These sensors hold immense promise across a spectrum of scenarios, encompassing ships, offshore engineering platforms, marine robots, and more. Within this section, we explore the extensive range of potential applications for marine whisker sensors, which can be broadly categorized into four main classes: marine structure monitoring, utilization in oceanographic instruments, enhancing tactile perception capabilities in marine robots, and facilitating non-contact environmental sensing in marine environments. We believe that this section can serve as a source of inspiration for researchers in the whisker sensor field, offering insights into the practical realization of these applications.

3.1. Marine Structure Monitoring

Marine structure monitoring encompasses the real-time or periodic assessment of diverse engineering structures, facilities, or natural phenomena situated in the ocean. These structures encompass offshore facilities, submarine cables, marine energy devices, marine bridges, marine platforms, ports, and offshore vessels, among others. Whisker sensors present many application prospects in monitoring marine structures [108–112]. They can establish contact with the structure's surface or its surrounding environment to capture the physical condition of the structure, thus enhancing the safety, reliability, and longevity of marine structures. Reeder et al. introduced a dense, highly sensitive, and multimodal electronic whisker sensing array constructed on a shape memory polymer substrate [113], as illustrated in Figure 8A,B. This array can detect proximity, microtexture, surface roughness, force, material rigidity, and temperature with a response time of less than 250 μ s. Electronic whiskers are fabricated from resistive sensors using planar lithography and transformed into shape-adjustable, deterministic 3D components using directed airflow at temperatures above the substrate's transition temperature, as shown in Figure 8C. This electronic whisker array can discern fingerprints and leather textures, with the texture mapping results aligning with those obtained using a profilometer. While this study did not delve deeply into its application in the field of marine structure monitoring, this versatile sensing array can be affixed to robotic arms or robots for surface damage detection on structures. Furthermore, its ability to sense force and temperature makes it suitable for extended monitoring of marine structures such as marine risers and ship pipelines.

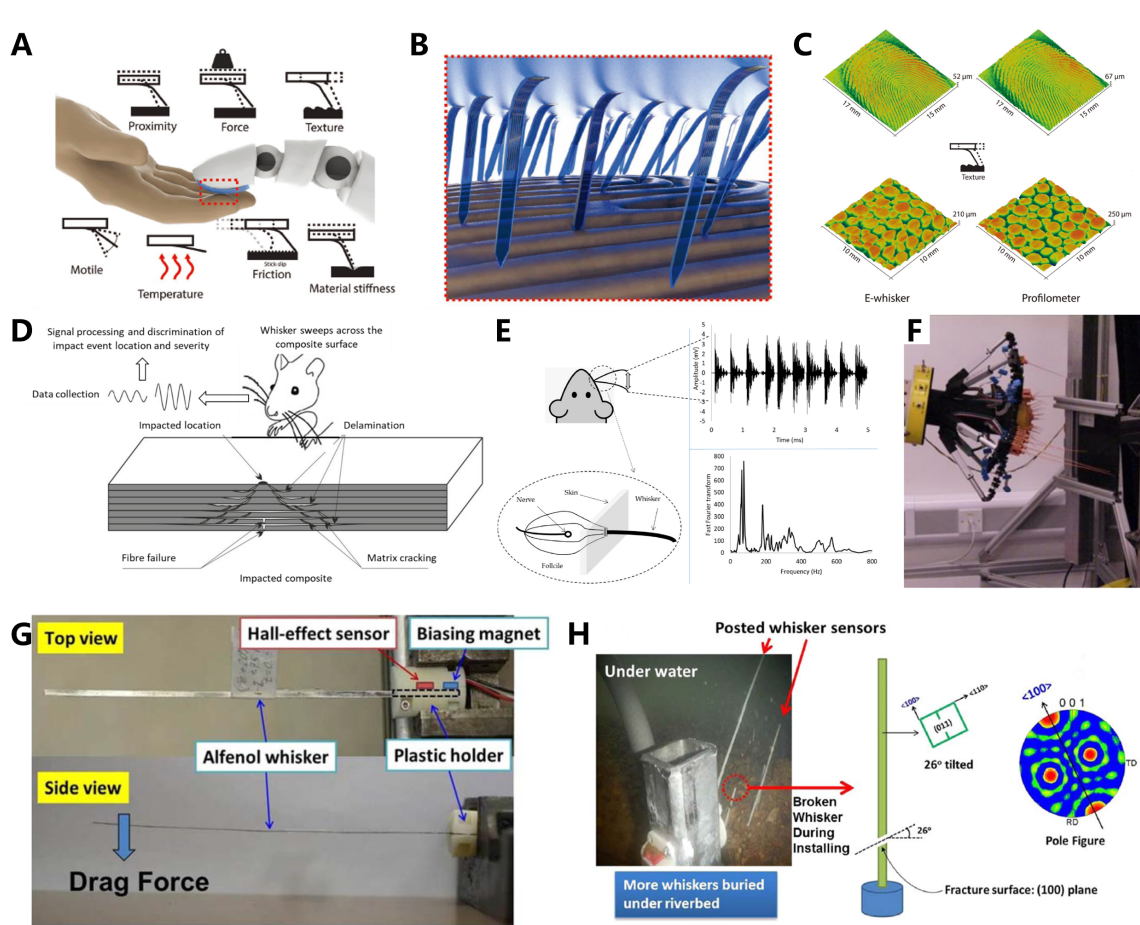


Figure 8. Marine structure monitoring. (A). Schematic diagram of the sensing modalities using 3D electronic whiskers. (B). Closeup illustration of an array of electronic whiskers interrogating a fingerprint. (C). Schematic diagram of the surface map of a fingerprint and a piece of leather constructed by e-whiskers and profilometer. (A–C) Reproduced with permission. Ref. [113] Copyright 2018, WILEY-VCH. (D). Schematic diagram of a typical damage mechanism in barely visible impact damage. (E). Schematic diagram of the typical transient signals obtained from the whisker sensor. (F). Physical picture of the whisker scanning setup. (D–F) Reproduced with permission. Ref. [63] Copyright 2021, MDPI. (G). Schematic diagram of the configuration of a magnetostrictive flow sensor module composed of magnetostrictive whisker. (H). Schematic diagram of the magnetostrictive whisker as scour sensor for bridge detection application. (G,H) Reproduced with permission. Ref. [62] Copyright 2018, IOP Publishing.

Fotouhi et al. introduced a method for detecting barely visible impact damage (BVID) in materials employing whisker sensors [63], as depicted in Figure 8D. BVID typically results from low-velocity impacts (LVI), such as foreign object impacts on submarine surfaces or structural damage during assembly or maintenance procedures. Detecting BVID is challenging through conventional visual inspection, yet it significantly impacts structural integrity. Their whisker sensor comprises a small motor driving whisker oscillations, 3D-printed whiskers, and Hall effect sensors. The sensing mechanism, as shown in Figure 8E, relies on the non-stationary frequency characteristics of intermittent contact between the whiskers and the structure’s surface. Classification feature vectors are derived through time-frequency analysis, and a support vector machine (SVM) classifier is trained for accurate classification. After 13 or more training sessions involving repeated, brief whisker contacts with test samples, close to 100% classification accuracy is achieved. Figure 8F displays the physical assembly of this sensing system, which detects BVID in samples through repeated, brief whisker contacts at their tips. Na et al. propose whisker sensors constructed

from Fe-Al (phenol) and Fe-Ga (gallium) rolled sheets with preferred orientations, serving effectively as flow sensors [62]. They respond to local variations in magnetization intensity induced by bending stress during fluid flow resistance, as shown in Figure 8G. These magnetization intensity changes are translated into electrical signal outputs employing Hall effect sensors. Notably, this sensor can be utilized as part of a bridge automatic scour monitoring system. Historically, bridge scour has been the leading cause of bridge failures. Figure 8H illustrates how this team, with support from the U.S. Department of Transportation (USDOT), deployed prototype scour sensor columns on a Maryland highway bridge equipped with flow sensors made of triphenyl whiskers. The findings of this research can also be applied to damage warning systems for offshore platforms or nearshore equipment to mitigate damage to marine structures under extreme conditions.

3.2. Marine Measuring Instruments

Marine measurement instruments encompass a range of devices and equipment employed for data collection and measurement in the marine environment. Whisker sensors, as miniature, integrated, and intelligent sensors, hold the potential to significantly enhance the sensing capabilities of existing systems, offering insights into multiple parameters, including velocity [114,115], viscosity [102], vibration [116], underwater acoustics [64,117,118], and more. Liu et al. devised a deployable Kirigami whisker sensor by combining Kirigami skin pop-up functionality with flexible conductive layers [119], as depicted in Figure 9A. This sensor transitions from a flat state to a sensing state, with adjustable whisker stiffness and initial pop-up angle achieved by tuning pre-stretch strain. It comprises Kirigami layers with printed conductive sensor layers. Kirigami, a 2D layer structure cut into specific patterns, transforms into 3D pop-up structures when subjected to strain. A trapezoidal pattern was chosen for its superior stretchability and larger pop-up angle. The experimental setup, presented in Figure 9B, serves as an underwater flow meter. As water flows over the whiskers, it induces bending deformation, detected by the conductive layer sensors. Figure 9C provides average resistance change rate data from three repeated experiments, divided by the standard deviation. The results indicate a linearly increasing relationship between resistance change rate and water flow rate.

Drawing inspiration from marine mammal tactile whiskers, Rooney et al. introduced a novel method for determining the relative viscosity density of fluids using driven flexible beams [120]. The sensor structure, displayed in Figure 9D, incorporates artificial whiskers based on the Hall effect sensor model, installed within follicle casings and connected to a PC for data sampling via a straightforward microcontroller interface. The whisker sensor generates two voltages proportional to the deflection degrees along two orthogonal axes of the whisker shafts. The voltage-to-deflection ratio is pre-programmed during assembly and calibrated using load sensors and micrometer displacement tools. A schematic of viscosity sensing tests is presented in Figure 9E. The whisker sensor, mounted on the spindle of a waterproof servo motor, rotates at a set angular velocity along an arc, with a glycerin and water mixture in the device. Adjusting the glycerin proportion alters fluid dynamic viscosity. As shown in Figure 9F, the output data reveal that higher viscosity fluids lead to an increased amplitude of re-entrant sensing response on both measurement axes. When immersed in viscous fluid, the whiskers undergo intrinsic frequency changes, allowing the whisker sensor to classify fluid viscosity through controlled stirring-induced self-motion modes.

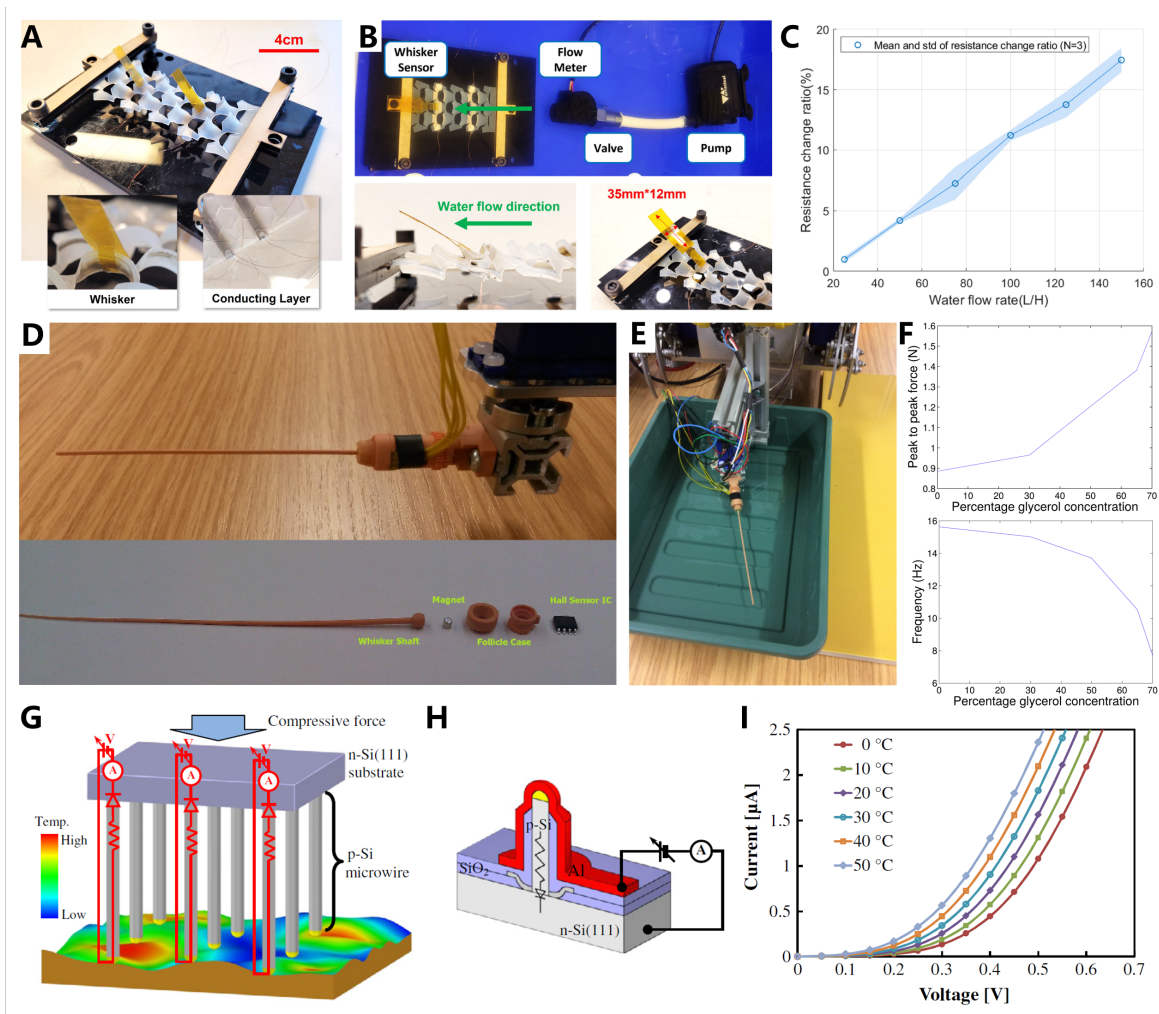


Figure 9. Marine measuring instruments. (A). Schematic diagram of the Kirigami whisker sensor. (B). Schematic diagram of the underwater test setup. (C). The test result of the relationship between resistance changing ratio versus water flow rate. (A–C) Reproduced with permission. Ref. [119] Copyright 2022, IEEE. (D). Schematic diagram of the assembled sensor mounted onto servo motor for whisker tank experiments and the details of the main components of the sensor assembly. (E). Schematic diagram of the whisker tank experimental configuration. (F). Schematic diagram of whisker signals in controlled viscosity. (D–F) Reproduced with permission. Ref. [120] Copyright 2015, Springer. (G). Schematic diagram of an artificial whisker array. (H). Schematic diagram of the cross-sectional device image of an individual whisker sensor. (I). Schematic diagram of the temperature sensitivity of the embedded p-n diode. (G–I) Reproduced with permission. Ref. [121] Copyright 2011, IOP Publishing.

Ikedo et al. introduced a planar out-of-plane high aspect ratio “whisker-like” micro-wire array sensor for multi-point contact force and temperature detection with high spatial resolution [121]. The sensor relies on vertically assembled piezoresistive p-type silicon micro-wires on an n-type silicon substrate catalyzed by selective VLS (vapor–liquid–solid method) growth of silicon, as shown in Figure 9G. VLS growth enables the creation of artificial whisker sensors with precisely defined wire diameter and position, based on integrated circuit (IC) photolithography. This precision results in high-density wire arrays and enables control of various lengths of out-of-plane wires at the micrometer to millimeter scale. Figure 9H displays a cross-sectional device image of a single whisker sensor element composed of piezoresistive p-type silicon VLS micro-wires assembled on an n-type silicon substrate, forming a p-type silicon wire/p-n diode system. Using the same sensor arrangement, piezoresistive silicon micro-wires and embedded p-n diodes can be employed for

force and temperature sensing, respectively. Figure 9I illustrates the I–V curve related to temperature for the wire/p-n diode measured under a forward bias voltage of 0 to 0.7 V. At forward bias voltages between 0.1 and 0.25 V, the forward current is primarily determined by the p-n diode characteristics. Leveraging this feature, the sensor achieves temperature detection capabilities with sub-second time resolution in microscale regions.

3.3. Marine Robot Tactile Perception

Tactile perception in marine robots encompasses the capacity to sense objects and surfaces within the environment through touch and pressure sensors, facilitating interactive engagement. Integration of whisker sensors with marine robots extends their functionality to address diverse application needs. For instance, whisker sensors enable distance and shape recognition, facilitating the development of tactile Simultaneous Localization and Mapping (SLAM) systems for cabin inspection robots [122–125]. This complements their limited optical perception capabilities in close proximity. Underwater robots, equipped with whisker sensors, gain tactile recognition capabilities, enabling the detection and identification of surrounding obstacles, thereby enhancing their operability. Wei et al. proposed a MEMS-based (MEMS, Micro-electromechanical Systems) biomimetic whisker sensor inspired by rodents, which integrates four sensing units on a square silicon wafer measuring 6.8 mm per side [126]. This design allows mounting on small robots similar in size to real rodents. The constructed mouse-like robot and sensor design are shown in Figure 10A. Due to its compact size, this robot exhibits high potential for applications in confined spaces on ships or in cabins. To mimic the mechanical receptors in whisker follicles, which perceive whisker deflection and measure torque at the whisker's base, the sensing unit comprises a whisker shaft, a central connector, and four beams. The whisker shaft is embedded within the central connector, and four piezoresistors are integrated into the beams arranged in a cross shape. These piezoresistors are configured in a Wheatstone bridge to convert changes in resistance values into electrical signals. The proposed prototype robot achieves distance measurement and surface shape recognition capabilities akin to those of real rodents, as illustrated in Figure 10B. As the whisker makes contact with a surface, the contact distance changes due to the varying curvatures of the recognized object's surface. Consequently, the shape of the sensor's output waveform reflects the shape of the contacted surface. Figure 10C displays the perception signals of the whisker sensor during sweeping movements on circular and flat surfaces, demonstrating how the sensor's time waveform reflects surface curvature.

Autonomous guided vehicles (AGVs) serve as viable choices for cabin or offshore platform inspection robots. An et al. designed a flexible biomimetic whisker mechanoreceptor (BWMR) inspired by the way animals employ hair-based sensors to explore their environment [127]. The BWMR utilizes triboelectric nanogenerator technology, allowing it to convert external mechanical stimuli into electrical signals without the need for an external power source. This feature makes it suitable for widespread use in robots. The BWMR facilitates the identification of objects that conventional environmental detection methods like vision and ultrasonic radar cannot detect, substantially expanding a robot's ability to gather information about its surroundings, as depicted in the application schematic in Figure 10D. The BWMR consists of 0.2 mm thick FEP strips, mimicking animal whiskers, and biomimetic follicles that encompass two metal electrodes. These biomimetic follicles encapsulate two electrodes of the TENG, helping to resist interference from the external environment. By integrating the BWMR into AGVs, it becomes possible to achieve automatic obstacle avoidance, as depicted in Figure 10E. A computer program analyzes the real-time output signals from the BWMR, enabling precise automatic obstacle avoidance based on the collision angle. The transfer charge signals obtained from two BWMR sensors during obstacle avoidance are shown in Figure 10F. When the sensor detects a collision signal, the robot swiftly takes evasive action, resulting in waveform characteristics that initially rise and then quickly fall.

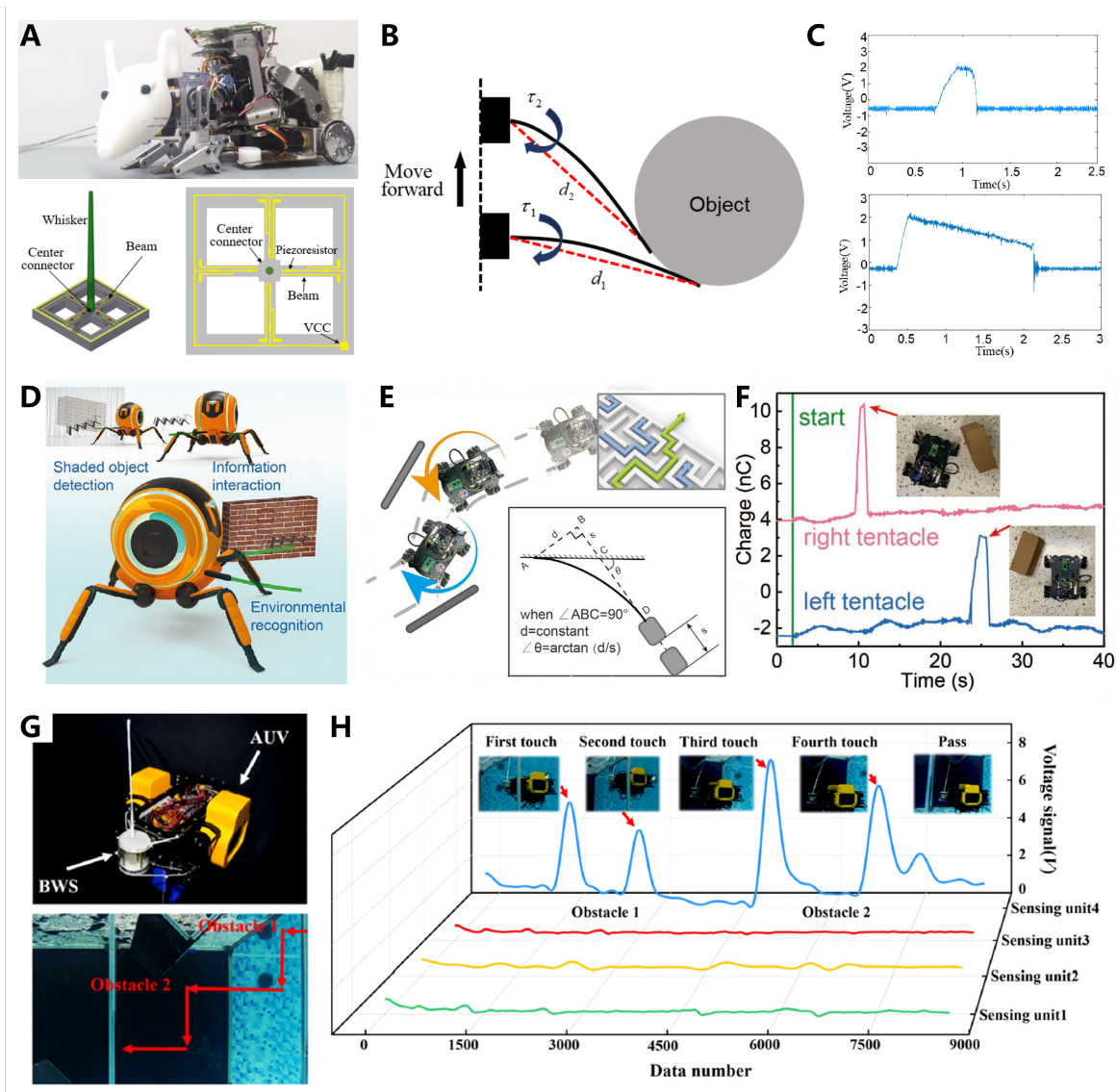


Figure 10. Marine robot tactile perception. (A). Schematic diagram of the robotic rat equipped with whisker sensor and the design method of whisker sensor. (B). Schematic diagram of the shape recognition. (C). Deflection signal of the whisker sensor sliding on surface of round and flat shape. (A–C) Reproduced with permission. Ref. [126] Copyright 2019, IEEE. (D). Application of the biomimetic whisker mechanoreceptors in shaded object detection, information interaction, and environment recognition for robotics. (E). Schematic diagram of the strategy and trajectory of the application of the biomimetic whisker mechanoreceptors in robotics for environment and obstacle recognition. (F). Real-time acquired transferred charge signals from the electrometer DAQ board in the process of autonomous obstacle avoidance. (D–F) Reproduced with permission. Ref. [127] Copyright 2021, WILEY-VCH. (G). Schematic diagram of the sensor configuration and experimental scene layout during reactive obstacle avoidance. (H). The output signal of bionic whisker sensor for underwater reactive obstacle avoidance. (G,H) Reproduced with permission. Ref. [67] Copyright 2022, Elsevier B.V. using BWS.

By ensuring the waterproofing and specialized design of whisker sensors, they can also be directly applied in underwater environments. Taking inspiration from sea otter whisker structures, Xu et al. designed a TENG-based biomimetic whisker sensor (BWS) to assist underwater robots in perceiving the underwater environment [65]. The sensing unit generates electrical signals through triboelectric effect and electrostatic induction between an FEP thin film and ink. A detailed discussion of its structure is provided in Section 2.6.

With a biologically inspired structural design, artificial BWS can estimate the external stimulus area. Integration of the BWS into the head of underwater robots enables obstacle avoidance based on BWS perception, as demonstrated in the physical diagram and obstacle configuration in Figure 10G. The underwater robot encounters obstacles in a water tunnel constructed from transparent acrylic plates measuring $1.6\text{ m} \times 0.8\text{ m} \times 0.8\text{ m}$. Obstacle 1 is positioned at the tunnel entrance, while obstacle 2 comprises three prisms affixed to the tunnel's upper wall. As the underwater robot progresses into the water tunnel, the BWS initially collides with the tunnel's upper wall, generating an electrical signal. Subsequently, the underwater robot adjusts its diving depth to navigate into the tunnel smoothly. When the BWS detects obstacle 2 within the tunnel, the underwater robot repeats the depth adjustment procedure to successfully navigate the obstacle. Figure 10H offers insight into the specific shape of the BWS and real-time voltage signals as the underwater robot avoids these two obstacles. The results illustrate that the underwater robot equipped with the BWS can effectively detect the surface conditions within the underwater tunnel and autonomously avoid obstacles.

3.4. Marine Non-Contact Environmental Sensing

The utilization of whisker sensors for non-contact environmental sensing in the marine environment represents an innovative approach. These specialized sensors draw inspiration from marine mammals and other animals' whiskers to gather information about the underwater environment without the necessity for direct physical contact. In contemporary research, the development of sensors geared towards achieving non-contact environmental sensing in the ocean is predominantly influenced by seal whiskers [128–131]. Extensive studies on the fluid dynamics associated with seal whiskers provide a robust theoretical underpinning for the design and implementation of whisker sensors for marine non-contact environmental perception. Zheng et al. introduced a fully 3D-printed MEMS cantilever sensor designed to experimentally measure the responses to vortex-induced vibration (VIV) and flow-induced vibration (WIV) in individual 3D-printed seal whiskers and arrays [68]. The structural diagram of the sensor and its assembly with 3D-printed seal whiskers are depicted in Figure 11A. This MEMS cantilever beam sensor is crafted through 3D printing, with pressure-sensitive resistors employing graphene nanomaterials embedded at the hinges. The 3D-printed seal whisker structures are integrated into 3D-printed whisker brackets and affixed to the distal end of the MEMS cantilever beam sensor. Notably, the parameters for the artificial whiskers in this study were extracted from 3D measurement data of the cross-sectional morphological characteristics of seal whiskers and gray seal whiskers. This represents a pioneering effort in creating 3D scans of seal whiskers. Schematics illustrating the measurement of VIV and WIV by whisker sensors are presented in Figure 11B. The results of these measurements affirm that seal whiskers vibrate at the WIV frequency, synchronized with the dominant frequency of the wake vortex. This provides robust theoretical support for the development and deployment of low-noise sensors applicable to underwater robots.

Eberhardt et al. devised a Wake Information Detection and Tracking System (WIDTS) founded on the capacitive whisker sensor proposed in Section 2.4 [95]. This system features multiple whisker-like elements capable of responding to hydrodynamic disturbances encountered during underwater locomotion. To evaluate whether the WIDTS sensor's capacity to detect underwater wake in laboratory settings can be extrapolated to dynamic testing environments akin to those encountered by biological models, the research team securely attached the WIDTS to occlusal plates within the seal's mouth. This exposed the sensor to a fluid dynamic environment reminiscent of free-swimming seals, as illustrated in Figure 11C. Chase experiments involving seals were recorded using a wide-angle camera positioned directly above the test pool, as demonstrated in Figure 11D. Remarkably, the seals consistently tracked the path left by the submarine, irrespective of whether they carried the WIDTS. Data from the WIDTS sensor, detailing the deflection angles of whisker elements as they traversed the fluid dynamic trajectory created by the submarine, are pre-

sented in Figure 11E. Video performance data corroborate that these detections correspond in time with WIDTS-wake intersections.

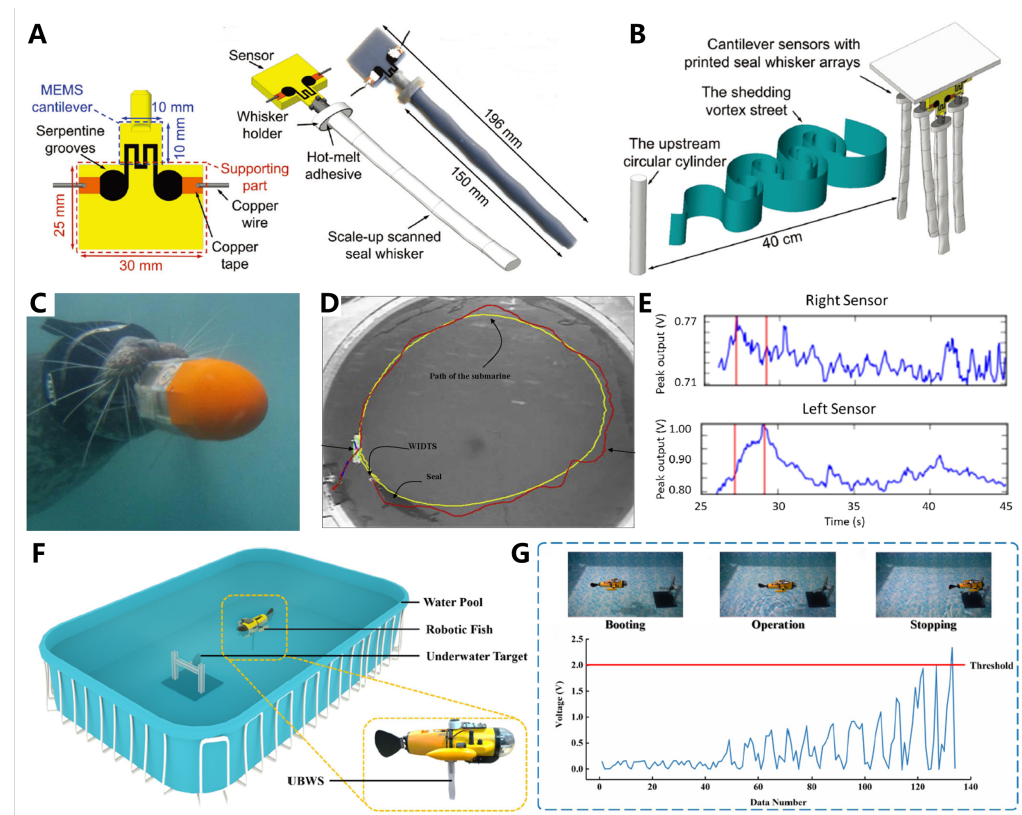


Figure 11. Marine non-contact environmental sensing. (A). Schematic diagram of the 3D-printed cantilever sensor and whisker vibration measurements in the recirculating water flume. (B). Schematic diagram of the diagrammatic sketch showing the seal whisker structure arrays in a wake generated by an upstream circular cylinder. (A,B) Reproduced with permission. Ref. [68] Copyright 2023, WILEY-VCH. (C). Schematic diagram of the harbor seal Sprouts tracking an underwater wake while wearing a blindfold and holding the Wake Information Detection and Tracking System firmly in his mouth. (D). Schematic diagram of a simple experimental trial. (E). The data Wake Information Detection and Tracking System with the screenshot times indicated by red lines. (C–E) Reproduced with permission. Ref. [95] Copyright 2016, IOP Publishing. (F). Schematic diagram of the experimental setup of the underwater bionic whisker sensor. (G). Three states during the movement of the robotic fish and corresponding voltage signal of the underwater bionic whisker sensor. (F,G) Reproduced with permission. Ref. [66] Copyright 2022, Elsevier B.V.

In a similar vein to seal whiskers, Wang et al. introduced a flexible biomimetic whisker sensor, distinct from the previously mentioned whisker sensors, denoted as the Underwater Biomimetic Whisker Sensor (UBWS) [66]. The UBWS comprises an internally autonomous layered triboelectric nanogenerator sensing unit, flexible silicone gel follicles (Dragonskin 00-20), and artificial whiskers (polydimethylsiloxane, PDMS). The follicles envelop the upper portion of the sensing unit, while the artificial whiskers cover the lower portion. The variation in material elasticity between the upper and lower halves of the UBWS culminates in the primary deflection point along the sensing unit, generating strain at the material junction. The UBWS is integrated into a robotic fish for the purpose of underwater target tracking, as depicted in Figure 11F. The experimental setup entails an indoor pool measuring 3 m × 2 m × 1.5 m, with the UBWS linked to an Arduino control module within the robotic fish via a data collection module. Control is achieved through a straightforward closed-loop control system, with the robotic fish’s movement classified into three states, as shown in Figure 11G. When the UBWS captures vortex information from underwater

targets, the robotic fish adjusts its course toward the target until the voltage signal reaches a preset threshold. This application demonstrates the feasibility of UBWS-based tracking of underwater targets even when visual cues are limited or absent. It is important to note that while flexible whisker structures enhance sensitivity, the strain processes involved are relatively intricate and may pose challenges in effectively elucidating them using existing theoretical models. Moreover, flexible structures introduce increased instability, potentially posing challenges in achieving effective sensing in practical applications.

As depicted in Table 1, this review intuitively outlines the categories, performance attributes, and potential applications of various whisker sensors. Optical whisker sensors pose a challenge in the realm of marine science and engineering due to the inherent complexity of their acquisition systems. Magnetic and resistive whisker sensors, having been developed earlier and subjected to in-depth scrutiny, yield a substantial body of research results with demonstrable application potential in the domain of marine science and engineering. On the other hand, capacitive whisker sensors confront limitations stemming from their susceptibility to environmental variations and high demands in packaging processes, impeding their broader utility in marine science and engineering applications. Despite a paucity of existing research outcomes, the prospective value of piezoelectric and triboelectric whisker sensors in the marine science and engineering arena cannot be discounted. Their robust environmental adaptability renders them particularly suited for underwater applications. Notably, triboelectric whisker sensors, characterized by a brief developmental history, harbor extensive research prospects and are poised to assume a pivotal role in shaping the future landscape of applications in the field of marine science and engineering.

Table 1. The categories, performance, and potential applications of various whisker sensors.

Category	Performance	Potential Applications	Reference
Magnetic	Response time of less than 0.88 s	Surface recognition	[108]
Magnetic	Accuracy level of almost 100%	Damage detecting	[63]
Magnetic	Scour monitoring at Maryland State Highway bridges	Scour monitoring	[62]
Magnetic	Success generally increases as flow rate increases	Scour monitoring	[109]
Magnetic	Frequency sensitive	Scour monitoring	[110]
Magnetic	Robustly classifying the viscosity of fluids	Viscometer	[120]
Magnetic	Root mean squared percentage error less than 3.96%	Flow meter	[114]
Magnetic	Force resolution 0.4 mN, spatial resolution 0.04 mm × 0.04 mm	Vibrometer	[116]
Resistive	Response time of less than 250 μs	Surface recognition	[113]
Resistive	Roughly check and estimate the surrounding flow rate	Flow meter	[119]
Resistive	Small detection area (~20 μm ²) and high spatial resolution (~100 μm in pitch)	Thermometer	[121]
Resistive	Recognize precision is as low as 0.2 m ³ s ⁻¹ within 0.1 s	Flow meter	[115]
Resistive	Sensitivities about −204.6 dB@300 Hz (X channel) and −210.2 dB@300 Hz (Y channel)	Hydrophone	[64]
Resistive	Resonance frequency of sensor is nearly 1450 Hz	Hydrophone	[117]
Resistive	Available bandwidth of sensor ranging from 20 to 500 Hz	Hydrophone	[118]
Resistive	Compensation error with only 20.385%	Robot tactile perception	[122]
Resistive	Scan the surface profile of touched objects	Robot tactile perception	[123]
Resistive	Simultaneous Localization and Mapping	Robot tactile perception	[124]
Resistive	Simultaneous Localization and Mapping	Robot tactile perception	[125]
Resistive	Trail tracking	Flow field perception	[68]
Resistive	Sensitivity of sensor in any direction is detectable and remarkably high (% ~1180)	Flow field perception	[130]
Resistive	Perceive intricate flow details	Flow field perception	[131]
Capacitive	Target tracking	Flow field perception	[95]
Piezoelectric	Mechanical impedance is correlated with roughness	Surface recognition	[111]
Piezoelectric	Measurement uncertainty is less than 0.60%	Viscometer	[102]
Piezoelectric	Determine obstacle distance	Robot tactile perception	[126]
Triboelectric	Shaded object detection and environment recognition	Robot tactile perception	[127]
Triboelectric	Simultaneous Localization and Mapping	Robot tactile perception	[65]
Triboelectric	Perceiving underwater environment and avoiding reactive obstacles	Robot tactile perception	[67]
Triboelectric	Passive vortex perception	Flow field perception	[66]

4. Challenges and Future Perspectives

Despite the considerable promise exhibited across various sectors, whisker sensors encounter several pressing challenges that demand immediate attention. Foremost among these challenges is the pursuit of heightened accuracy and resolution. Despite ongoing research efforts aimed at augmenting the sensing precision and resolution of whisker sensors, they still lag behind conventional sensors such as cameras and laser radar in terms of performance. Furthermore, the applicability of whisker sensors remains relatively confined, primarily facilitating close-range sensing. While biological whiskers excel at long-range sensing, current research endeavors have struggled to match the prowess of biological counterparts. Artificial components within whisker sensors may be vulnerable to environmental factors, potentially compromising sensing stability and necessitating frequent recalibration. This also increases maintenance demands to protect against the adverse effects of wear and tear on the whisker's sensing effectiveness. Furthermore, the data output from whisker sensors tends to be complex, requiring extensive processing and analysis to extract feature information. Consequently, this places greater demands on signal acquisition and processing. Despite extant research concerning the utilization of whisker sensors in marine contexts, the extent of their integration remains relatively circumscribed. For instance, the direct acquisition of output signals from a whisker sensor is hindered by the precision limitations of current microcomputers. Numerous whisker sensors harboring substantial potential applications remain untapped in marine applications. To address these shortcomings, we propose future development directions for marine whisker sensors as follows:

(1) **In-depth Research into Whisker Sensing Theory:** The existing landscape of whisker sensors divides them into rigid and flexible categories based on the properties of artificial whisker materials. Rigid whisker sensors boast simpler structures, facilitating the establishment of sensing models; however, they often fall short in terms of performance. In contrast, flexible sensors exhibit superior sensitivity but frequently entail intricate strain processes, typically simplified into two-dimensional models for analytical purposes, rendering them theoretically less mature. Consequently, the ongoing pursuit revolves around the development of dependable mechanical models for artificial whiskers. The creation of robust theoretical models founded on well-established theory can underpin the design and fabrication of whisker sensors, curtailing trial-and-error costs. Simultaneously, the intricacies of the marine environment can be streamlined through further exploration of the fluid-structure coupling mechanism between whiskers and fluids.

(2) **Enhancing Sensing Capabilities:** The capabilities of whisker sensors pivot primarily on their design and materials. The sensing mechanism is heavily influenced by design configuration, making the optimization of design crucial to enhance sensing capabilities. Additionally, the material properties of the sensor not only impact the accuracy of artificial whiskers but also define the capacities of the sensing unit. For instance, in the case of triboelectric whisker sensors, improving the charging performance of both the dielectric layer and the electrodes within the sensing unit is a pivotal step towards enhancing sensing capabilities. The amelioration of artificial whisker materials can concurrently fortify their durability and stability, warranting intensified research efforts in the materials domain. Furthermore, the adept analysis of whisker sensor output signals is imperative for the enhancement of their sensing capabilities. By subjecting the sensor output signal to advanced techniques such as the Fast Fourier Transform or machine learning algorithms, it becomes possible to extract more pertinent feature information. Consequently, this leads to a substantial enhancement of their perceptual capabilities.

(3) **Developing Long-Term Monitoring and Autonomous Operation:** The marine milieu presents unique challenges concerning energy supply. Mitigating sensor energy consumption to enable protracted monitoring or autonomous data collection capabilities emerges as a critical imperative for sustained marine research. Current research endeavors have extended into the domain of self-powered sensing technologies, which include the utilization of piezoelectric or triboelectric nanogenerator technologies. These advancements

enable sensors to function autonomously, without reliance on external power sources. The exploration of their integration with whisker sensors presents a promising avenue for addressing this challenge. Furthermore, harnessing energy derived from the marine environment to power sensors offers a feasible solution. The reliability of whisker sensors is crucial for ensuring their long-term monitoring and automatic operation. An important aspect of assessing reliability involves evaluating metrics, including sensitivity, repeatability, and precision. Sensitivity is responsible for a sensor's capability to detect subtle environmental changes, while repeatability and precision gauge the consistency and accuracy of these measurements. These metrics are pivotal in determining the reliability of bionic whisker sensors in capturing and interpreting sensory data. A comparative analysis with other tactile sensing technologies can elucidate the strengths and weaknesses of whisker sensors in terms of reliability. Ongoing research and development efforts are directed toward enhancing materials, design, and signal processing techniques to bolster the reliability of these sensors across diverse applications.

(4) **Integration and Intelligence:** Whisker sensors, classified as tactile sensing technologies, harmonize seamlessly with other sensory modalities like sonar, cameras, and LiDAR (Light Detection And Ranging), culminating in multi-sensor fusion systems that augment overall marine perception in terms of comprehensiveness and precision. For instance, amalgamating whisker sensors with optical sensing apparatuses on underwater robots confers synchronous perception of the surrounding environment, encompassing far-field and near-field scenarios. This synergy enables superior detection and tracking of marine entities and structures. Additionally, the infusion of intelligent algorithms, such as deep learning and machine learning, can heighten real-time analysis and processing competencies concerning whisker sensor output data. This can ultimately culminate in automatic feature recognition, anomaly detection, and even prognostication of alterations in detected targets. The integration of whisker sensors with artificial intelligence represents an effective strategy to enhance sensing capabilities, enabling autonomous decision-making and control based on data collection.

(5) **Multidisciplinary Cross-Integration:** Whisker sensors inherently epitomize the product of interdisciplinary research. Their deeper exploration across various disciplines assumes pivotal significance in ameliorating their performance and broadening their horizons with regard to application areas. In the realm of materials science, the optimization or invention of new materials requisite for whisker sensors assumes centrality. Within the domain of mechanical design, inventive approaches can be pursued to ensure sensor robustness and stability. In the purview of biology, a deeper comprehension of the sensory mechanisms underpinning biological whiskers can serve as a fount of inspiration for whisker sensor designs. The field of data analysis and algorithm development requires the creation of intelligent algorithms designed to process and analyze sensor output data. In the realm of physics, the formulation of effective models and analyses relevant to whisker sensors can contribute to the refinement of theoretical models. For example, the incorporation of Internet of Things (IoT) technology with whisker sensors in the domains of marine science and engineering offers an abundance of data and diverse applications in the realms of environmental monitoring, marine biology research, navigation, security, aquaculture, and disaster response. Multidisciplinary integration not only advances whisker sensor technology but also facilitates its integration into these domains, promoting mutual growth across diverse disciplines. These envisioned future directions represent potential avenues for mitigating the current limitations associated with whisker sensors and pave the path for their ongoing development and application within the marine domain.

5. Conclusions

This review offered a comprehensive exploration of diverse categories of whisker sensors, encompassing optical, magnetic, resistive, capacitive, piezoelectric, and triboelectric variants. Furthermore, it provided insights into the varied potential applications of whisker sensors in the marine domain, classifying them into four distinct domains: marine structure

monitoring, marine measurement instruments, marine robot tactile perception, and marine non-contact environmental sensing. The challenges faced by whisker sensors in the fields of marine science and engineering, alongside their future prospects, underwent a thorough examination. The future prospects centered on five development directions: in-depth research into whisker sensing theory, enhancement of sensing capabilities, establishment of long-term monitoring and autonomous functionality, integration and intelligent systems, and multidisciplinary cross-integration. Although whisker sensors currently have limited applications in marine science and engineering, their substantial potential value in this field should not be underestimated.

Author Contributions: Writing—original draft preparation, S.W. and J.L.; investigation: B.L.; resources: H.W. and J.S.; writing—review and editing, P.X. and M.X. All authors have read and agreed to the published version of the manuscript.

Funding: This work was supported by the National Natural Science Foundation of China (52371345, 52101382), Dalian Outstanding Young Scientific and Technological Talents Project (2021RJ11), Application Research Program of Liaoning Province (2022JH2/101300219).

Institutional Review Board Statement: Not applicable.

Informed Consent Statement: Not applicable.

Data Availability Statement: No new data were created.

Conflicts of Interest: The authors declare no conflict of interest.

Abbreviations

The following abbreviations are used in this manuscript:

ROV	Remotely Operated Vehicles
SCF	Seven-core optical Fiber
PDMS	Polydimethylsiloxane
PCB	Printed Circuit Board
PLA	Polylactic Acid
PVDF	Polyvinylidene Difluoride
PZT	Lead Zirconium Titanate
TENG	Triboelectric Nanogenerator
FEP	Fluorinated Ethylene Propylene
CPP	Cast Polypropylene
BVID	Barely Visible Impact Damage
LVI	Low-velocity Impact
SVM	Support Vector Machine
USDOT	U.S. Department of Transportation
VLS	Vapor–liquid–solid method
IC	Integrated Circuit
SLAM	Simultaneous Localization and Mapping
MEMS	Micro-electromechanical Systems
AGV	Autonomous Guided Vehicle
BWMR	Biomimetic Whisker Mechanoreceptor
BWS	Bionic Whisker Sensor
VIV	Vortex-induced Vibration
WIV	Flow-induced Vibration
WIDTS	Wake Information Detection and Tracking System
UBWS	Underwater Bionic Whisker Sensor
LiDAR	Light Detection And Ranging
IoT	Internet of Things

References

- Spencer, B., Jr.; Ruiz-Sandoval, M.E.; Kurata, N. Smart sensing technology: Opportunities and challenges. *Struct. Control Health Monit.* **2004**, *11*, 349–368.
- Sladen, A.; Rivet, D.; Ampuero, J.P.; De Barros, L.; Hello, Y.; Calbris, G.; Lamare, P. Distributed sensing of earthquakes and ocean-solid Earth interactions on seafloor telecom cables. *Nat. Commun.* **2019**, *10*, 5777. [[PubMed](#)]
- Gao, W.; Emaminejad, S.; Nyein, H.Y.Y.; Challa, S.; Chen, K.; Peck, A.; Fahad, H.M.; Ota, H.; Shiraki, H.; Kiriya, D.; et al. Fully integrated wearable sensor arrays for multiplexed in situ perspiration analysis. *Nature* **2016**, *529*, 509–514. [[PubMed](#)]
- Zhang, H.; Gui, F. The Application and Research of New Digital Technology in Marine Aquaculture. *J. Mar. Sci. Eng.* **2023**, *11*, 401.
- Mohsan, S.A.H.; Li, Y.; Sadiq, M.; Liang, J.; Khan, M.A. Recent Advances, Future Trends, Applications and Challenges of Internet of Underwater Things (IoUT): A Comprehensive Review. *J. Mar. Sci. Eng.* **2023**, *11*, 124.
- Campagnaro, F.; Steinmetz, F.; Renner, B.C. Survey on Low-Cost Underwater Sensor Networks: From Niche Applications to Everyday Use. *J. Mar. Sci. Eng.* **2023**, *11*, 125.
- Wilson, J.S. *Sensor Technology Handbook*; Elsevier: Amsterdam, The Netherlands, 2004.
- Chaste, J.; Eichler, A.; Moser, J.; Ceballos, G.; Rurali, R.; Bachtold, A. A nanomechanical mass sensor with yoctogram resolution. *Nat. Nanotechnol.* **2012**, *7*, 301–304.
- Bayley, H.; Cremer, P.S. Stochastic sensors inspired by biology. *Nature* **2001**, *413*, 226–230.
- Kang, D.; Pikhitsa, P.V.; Choi, Y.W.; Lee, C.; Shin, S.S.; Piao, L.; Park, B.; Suh, K.Y.; Kim, T.I.; Choi, M. Ultrasensitive mechanical crack-based sensor inspired by the spider sensory system. *Nature* **2014**, *516*, 222–226.
- Sabri, N.; Aljunid, S.; Salim, M.; Ahmad, R.B.; Kamaruddin, R. Toward optical sensors: Review and applications. *J. Phys. Conf. Ser.* **2013**, *423*, 012064.
- Breazeal, C.; Scassellati, B. Robots that imitate humans. *Trends Cogn. Sci.* **2002**, *6*, 481–487. [[CrossRef](#)] [[PubMed](#)]
- Kundu, T. Acoustic source localization. *Ultrasonics* **2014**, *54*, 25–38. [[CrossRef](#)] [[PubMed](#)]
- Akyildiz, I.F.; Pompili, D.; Melodia, T. Underwater acoustic sensor networks: Research challenges. *Ad Hoc Netw.* **2005**, *3*, 257–279. [[CrossRef](#)]
- Tiwana, M.I.; Redmond, S.J.; Lovell, N.H. A review of tactile sensing technologies with applications in biomedical engineering. *Sens. Actuators A Phys.* **2012**, *179*, 17–31.
- Dahiya, R.S.; Metta, G.; Valle, M.; Sandini, G. Tactile sensing—From humans to humanoids. *IEEE Trans. Robot.* **2009**, *26*, 1–20. [[CrossRef](#)]
- Yang, T.; Xie, D.; Li, Z.; Zhu, H. Recent advances in wearable tactile sensors: Materials, sensing mechanisms, and device performance. *Mater. Sci. Eng. Rep.* **2017**, *115*, 1–37.
- Yousef, H.; Boukallel, M.; Althoefer, K. Tactile sensing for dexterous in-hand manipulation in robotics—A review. *Sens. Actuators A Phys.* **2011**, *167*, 171–187.
- Jones, L.A.; Sarter, N.B. Tactile displays: Guidance for their design and application. *Hum. Factors* **2008**, *50*, 90–111. [[CrossRef](#)]
- Fettweis, G.P. The tactile internet: Applications and challenges. *IEEE Veh. Technol. Mag.* **2014**, *9*, 64–70. [[CrossRef](#)]
- Lewis, P.M.; Ackland, H.M.; Lowery, A.J.; Rosenfeld, J.V. Restoration of vision in blind individuals using bionic devices: A review with a focus on cortical visual prostheses. *Brain Res.* **2015**, *1595*, 51–73.
- Pearson, M.J.; Mitchinson, B.; Sullivan, J.C.; Pipe, A.G.; Prescott, T.J. Biomimetic vibrissal sensing for robots. *Philos. Trans. R. Soc. B Biol. Sci.* **2011**, *366*, 3085–3096. [[CrossRef](#)] [[PubMed](#)]
- Li, W.; Pei, Y.; Zhang, C.; Kottapalli, A.G.P. Bioinspired designs and biomimetic applications of triboelectric nanogenerators. *Nano Energy* **2021**, *84*, 105865. [[CrossRef](#)]
- Yang, Y.; Song, X.; Li, X.; Chen, Z.; Zhou, C.; Zhou, Q.; Chen, Y. Recent progress in biomimetic additive manufacturing technology: From materials to functional structures. *Adv. Mater.* **2018**, *30*, 1706539. [[CrossRef](#)] [[PubMed](#)]
- Sayegh, M.A.; Daraghma, H.; Mekid, S.; Bashmal, S. Review of recent bio-inspired design and manufacturing of whisker tactile sensors. *Sensors* **2022**, *22*, 2705. [[CrossRef](#)]
- Beem, H.R.; Triantafyllou, M.S. Wake-induced ‘slaloming’ response explains exquisite sensitivity of seal whisker-like sensors. *J. Fluid Mech.* **2015**, *783*, 306–322. [[CrossRef](#)]
- Scholz, G.R.; Rahn, C.D. Profile sensing with an actuated whisker. *IEEE Trans. Robot. Autom.* **2004**, *20*, 124–127. [[CrossRef](#)]
- Wijaya, J.A.; Russell, R.A. Object exploration using whisker sensors. In Proceedings of the 2002 Australasian Conference on Robotics and Automation, Auckland, New Zealand, 27–29 November 2002; Australian Robotics and Automation Association (ARAA), Sydney, NSW, Australia, 2002; pp. 180–185.
- Grant, R.A.; Mitchinson, B.; Fox, C.W.; Prescott, T.J. Active touch sensing in the rat: Anticipatory and regulatory control of whisker movements during surface exploration. *J. Neurophysiol.* **2009**, *101*, 862–874. [[CrossRef](#)]
- Hartmann, M.J. Active sensing capabilities of the rat whisker system. *Auton. Robot.* **2001**, *11*, 249–254. [[CrossRef](#)]
- Diamond, M.E.; Von Heimendahl, M.; Knutsen, P.M.; Kleinfeld, D.; Ahissar, E. ‘Where’ and ‘what’ in the whisker sensorimotor system. *Nat. Rev. Neurosci.* **2008**, *9*, 601–612. [[CrossRef](#)]
- Diamond, M.E.; Arabzadeh, E. Whisker sensory system—From receptor to decision. *Prog. Neurobiol.* **2013**, *103*, 28–40. [[CrossRef](#)]
- Dehnhardt, G.; Mauck, B.; Bleckmann, H. Seal whiskers detect water movements. *Nature* **1998**, *394*, 235–236. [[CrossRef](#)]
- Zheng, X.; Kamat, A.M.; Cao, M.; Kottapalli, A.G.P. Creating underwater vision through wavy whiskers: A review of the flow-sensing mechanisms and biomimetic potential of seal whiskers. *J. R. Soc. Interface* **2021**, *18*, 20210629. [[CrossRef](#)] [[PubMed](#)]

35. Hirose, S.; Inoue, S.; Yoneda, K. The whisker sensor and the transmission of multiple sensor signals. *Adv. Robot.* **1989**, *4*, 105–117. [[CrossRef](#)]
36. Prescott, T.J.; Pearson, M.J.; Mitchinson, B.; Sullivan, J.C.W.; Pipe, A.G. Whisking with robots. *IEEE Robot. Autom. Mag.* **2009**, *16*, 42–50. [[CrossRef](#)]
37. Hires, S.A.; Pammer, L.; Svoboda, K.; Golomb, D. Tapered whiskers are required for active tactile sensation. *eLife* **2013**, *2*, e01350. [[CrossRef](#)]
38. Russell, R.A. Using tactile whiskers to measure surface contours. In Proceedings of the 1992 IEEE International Conference on Robotics and Automation, Nice, France, 12–14 May 1992; pp. 1295–1296.
39. Bovet, S.; Fend, M.; Pfeifer, R. Simulating whisker sensors—On the role of material properties for morphology, behavior and evolution. In *Proceedings of the 8th International Conference on the Simulation of Adaptive Behavior*; MIT Press: Cambridge, MA, USA, 2004; pp. 122–130.
40. Prescott, T.J.; Diamond, M.E.; Wing, A.M. Active touch sensing. *Philos. Trans. R. Soc. Lond. B Biol. Sci.* **2011**, *366*, 2989–2995. [[CrossRef](#)]
41. Solomon, J.H.; Hartmann, M.J. Artificial whiskers suitable for array implementation: Accounting for lateral slip and surface friction. *IEEE Trans. Robot.* **2008**, *24*, 1157–1167. [[CrossRef](#)]
42. Harada, S.; Honda, W.; Arie, T.; Akita, S.; Takei, K. Fully printed, highly sensitive multifunctional artificial electronic whisker arrays integrated with strain and temperature sensors. *ACS Nano* **2014**, *8*, 3921–3927. [[CrossRef](#)]
43. Ding, L.; Wang, Y.; Sun, C.; Shu, Q.; Hu, T.; Xuan, S.; Gong, X. Three-dimensional structured dual-mode flexible sensors for highly sensitive tactile perception and noncontact sensing. *ACS Appl. Mater. Interfaces* **2020**, *12*, 20955–20964. [[CrossRef](#)]
44. Lei, K.C.; Sou, K.W.; Chan, W.S.; Yan, J.; Ping, S.; Peng, D.; Ding, W.; Zhang, X.P. WSTac: Interactive Surface Perception based on Whisker-Inspired and Self-Illuminated Vision-Based Tactile Sensor. *arXiv* **2023**, arXiv:2308.13241.
45. Tuna, C.; Jones, D.L.; Kamalabadi, F. Tactile soft-sparse mean fluid-flow imaging with a robotic whisker array. *Bioinspir. Biomim.* **2015**, *10*, 046018. [[CrossRef](#)] [[PubMed](#)]
46. Wu, Z.; Ai, J.; Ma, Z.; Zhang, X.; Du, Z.; Liu, Z.; Chen, D.; Su, B. Flexible out-of-plane wind sensors with a self-powered feature inspired by fine hairs of the spider. *ACS Appl. Mater. Interfaces* **2019**, *11*, 44865–44873. [[CrossRef](#)] [[PubMed](#)]
47. Tiwana, M.I.; Tiwana, M.I.; Redmond, S.J.; Lovell, N.H.; Iqbal, J. Bio-inspired PVDF-based, mouse whisker mimicking, tactile sensor. *Appl. Sci.* **2016**, *6*, 297. [[CrossRef](#)]
48. Bebek, O.; Cavusoglu, M.C. Whisker sensor design for three dimensional position measurement in robotic assisted beating heart surgery. In Proceedings of the 2007 IEEE International Conference on Robotics and Automation, Rome, Italy, 10–14 April 2007; pp. 225–231.
49. Glick, R.; Muthuramalingam, M.; Brücker, C. Fluid-structure interaction of flexible whisker-type beams and its implications for flow sensing by pair-wise correlation. *Fluids* **2021**, *6*, 102. [[CrossRef](#)]
50. Zhang, X.; Shan, X.; Xie, T.; Miao, J.; Du, H.; Song, R. Harbor seal whisker inspired self-powered piezoelectric sensor for detecting the underwater flow angle of attack and velocity. *Measurement* **2021**, *172*, 108866. [[CrossRef](#)]
51. Rooney, T.; Pearson, M.; Welsby, J.; Horsfield, I.; Sewell, R.; Dogramadzi, S. Artificial active whiskers for guiding underwater autonomous walking robots. In Proceedings of the CLAWAR 2011, Paris, France, 6–8 September 2011.
52. Wang, S.; Xu, P.; Wang, X.; Wang, H.; Liu, C.; Song, L.; Xie, G.; Xu, M. Bionic tactile sensor based on triboelectric nanogenerator for motion perception. In Proceedings of the 2021 IEEE 16th International Conference on Nano/Micro Engineered and Molecular Systems (NEMS), Xiamen, China, 25–29 April 2021; pp. 1853–1857.
53. y Alvarado, P.V.; Bhat, S. Whisker-like sensors with tunable follicle sinus complex for underwater applications. In Proceedings of the Bioinspiration, Biomimetics, and Bioreplication 2014, San Diego, CA, USA, 9–12 March 2014; Volume 9055, pp. 79–88.
54. Wegiriya, H.; Herzig, N.; Abad, S.A.; Sadati, S.H.; Nanayakkara, T. A stiffness controllable multimodal whisker sensor follicle for texture comparison. *IEEE Sens. J.* **2019**, *20*, 2320–2328. [[CrossRef](#)]
55. Russell, R.A.; Wijaya, J.A. Object location and recognition using whisker sensors. In Proceedings of the Australasian Conference on Robotics and Automation, Sydney, NSW, Australia, 1–3 December 2003; pp. 761–768.
56. Fox, C.; Evans, M.; Pearson, M.; Prescott, T. Tactile SLAM with a biomimetic whiskered robot. In Proceedings of the 2012 IEEE International Conference on Robotics and Automation, Saint Paul, MN, USA, 14–18 May 2012; pp. 4925–4930.
57. Zhang, Z.; Zhang, C.; Zuo, S. A Novel Bioinspired Whisker Sensor for Gastrointestinal Endoscopy. *IEEE/ASME Trans. Mechatron.* **2023**, 1–11. [[CrossRef](#)]
58. Kent, T.A.; Emnett, H.; Babaei, M.; Hartmann, M.J.; Bergbreiter, S. Identifying Contact Distance Uncertainty in Whisker Sensing with Tapered, Flexible Whiskers. In Proceedings of the 2023 IEEE International Conference on Robotics and Automation (ICRA), London, UK, 29 May–2 June 2023; pp. 607–613.
59. Toal, D.J.; Flanagan, C.; Lyons, W.B.; Nolan, S.; Lewis, E. Proximal object and hazard detection for autonomous underwater vehicle with optical fibre sensors. *Robot. Auton. Syst.* **2005**, *53*, 214–229. [[CrossRef](#)]
60. Deer, W.; Pounds, P.E. Lightweight whiskers for contact, pre-contact, and fluid velocity sensing. *IEEE Robot. Autom. Lett.* **2019**, *4*, 1978–1984. [[CrossRef](#)]
61. Beem, H.; Hildner, M.; Triantafyllou, M. Calibration and validation of a harbor seal whisker-inspired flow sensor. *Smart Mater. Struct.* **2012**, *22*, 014012. [[CrossRef](#)]

62. Na, S.; Park, J.; Jones, N.; Werely, N.; Flatau, A. Magnetostrictive whisker sensor application of carbon fiber-alfenol composites. *Smart Mater. Struct.* **2018**, *27*, 105010. [[CrossRef](#)]
63. Fotouhi, S.; Khayatzadeh, S.; Pui, W.X.; Damghani, M.; Bodaghi, M.; Fotouhi, M. Detection of barely visible impact damage in polymeric laminated composites using a biomimetic tactile whisker. *Polymers* **2021**, *13*, 3587. [[CrossRef](#)] [[PubMed](#)]
64. Bai, B.; Ren, Z.; Ding, J.; Xu, W.; Zhang, G.; Liu, J.; Zhang, W.; Xue, C.; Zhang, B.; Wang, R. Cross-supported planar MEMS vector hydrophone for high impact resistance. *Sens. Actuators A Phys.* **2017**, *263*, 563–570. [[CrossRef](#)]
65. Xu, P.; Wang, X.; Wang, S.; Chen, T.; Liu, J.; Zheng, J.; Li, W.; Xu, M.; Tao, J.; Xie, G. A triboelectric-based artificial whisker for reactive obstacle avoidance and local mapping. *Research* **2021**, *2021*, 9864967. [[CrossRef](#)]
66. Wang, S.; Xu, P.; Wang, X.; Zheng, J.; Liu, X.; Liu, J.; Chen, T.; Wang, H.; Xie, G.; Tao, J.; et al. Underwater bionic whisker sensor based on triboelectric nanogenerator for passive vortex perception. *Nano Energy* **2022**, *97*, 107210. [[CrossRef](#)]
67. Liu, J.; Xu, P.; Zheng, J.; Liu, X.; Wang, X.; Wang, S.; Guan, T.; Xie, G.; Xu, M. Whisker-inspired and self-powered triboelectric sensor for underwater obstacle detection and collision avoidance. *Nano Energy* **2022**, *101*, 107633. [[CrossRef](#)]
68. Zheng, X.; Kamat, A.M.; Cao, M.; Kottapalli, A.G.P. Wavy Whiskers in Wakes: Explaining the Trail-Tracking Capabilities of Whisker Arrays on Seal Muzzles. *Adv. Sci.* **2023**, *10*, 2203062. [[CrossRef](#)]
69. Zhang, P.; Wang, S.; Jiang, J.; Li, Z.; Yang, H.; Dai, X.; Liu, T. A Fiber-Optic Extrinsic Fabry–Perot Hydrophone Based on Archimedes Spiral-Type Sensitive Diaphragm. *IEEE Sens. J.* **2022**, *22*, 22654–22660. [[CrossRef](#)]
70. Lepora, N.F. Biomimetic active touch with fingertips and whiskers. *IEEE Trans. Haptics* **2016**, *9*, 170–183. [[CrossRef](#)]
71. Zhao, C.; Jiang, Q.; Li, Y. A novel biomimetic whisker technology based on fiber Bragg grating and its application. *Meas. Sci. Technol.* **2017**, *28*, 095104. [[CrossRef](#)]
72. Wang, J.; Yang, X.; Wang, A.; Jiang, H.; Bai, L.; Meng, H.; Li, S.; Geng, T.; Sun, W. Bio-Inspired Fiber Attitude Sensor for Direction-Distinguishable Pitching and Rolling Sensing. *J. Light. Technol.* **2023**, *41*, 6844–6851. [[CrossRef](#)]
73. Kent, T.A.; Kim, S.; Kornilowicz, G.; Yuan, W.; Hartmann, M.J.; Bergbreiter, S. WhiskSight: A reconfigurable, vision-based, optical whisker sensing array for simultaneous contact, airflow, and inertia stimulus detection. *IEEE Robot. Autom. Lett.* **2021**, *6*, 3357–3364. [[CrossRef](#)]
74. Lepora, N.F.; Pearson, M.; Cramphorn, L. TacWhiskers: Biomimetic optical tactile whiskered robots. In *Proceeding of the 2018 IEEE/RSJ International Conference on Intelligent Robots and Systems (IROS)*, Madrid, Spain, 1–5 October 2018; pp. 7628–7634.
75. Kim, S.; Velez, C.; Patel, D.K.; Bergbreiter, S. A magnetically transduced whisker for angular displacement and moment sensing. In *Proceedings of the 2019 IEEE/RSJ International Conference on Intelligent Robots and Systems (IROS)*, Macau, China, 3–8 November 2019; pp. 665–671.
76. Zhao, R.; Lu, Q.G.; Cao, Q. Magnetostrictive bioinspired whisker sensor based on galfenol composite cantilever beam realizing bidirectional tactile perception. *Appl. Bionics Biomech.* **2018**, *2018*, 4250541. [[CrossRef](#)]
77. Kim, D.; Möller, R. Passive sensing and active sensing of a biomimetic whisker. In *Proceedings of the International Conference on the Simulation and Synthesis of Living Systems*, Bloomington, IN, USA, 3–6 June 2006; Indiana University Press: Bloomington, IN, USA, 2006; pp. 127–131.
78. Volkova, T.; Böhm, V.; Naletova, V.; Kaufhold, T.; Becker, F.; Zeidis, I.; Zimmermann, K. A ferrofluid based artificial tactile sensor with magnetic field control. *J. Magn. Magn. Mater.* **2017**, *431*, 277–280. [[CrossRef](#)]
79. Kim, S.; Kubicek, R.; Paris, A.; Tagliabue, A.; How, J.P.; Bergbreiter, S. A whisker-inspired fin sensor for multi-directional airflow sensing. In *Proceedings of the 2020 IEEE/RSJ International Conference on Intelligent Robots and Systems (IROS)*, Las Vegas, NV, USA, 24 October–24 January 2020; pp. 1330–1337.
80. Yu, Z.; Sadati, S.H.; Perera, S.; Hauser, H.; Childs, P.R.; Nanayakkara, T. Tapered whisker reservoir computing for real-time terrain identification-based navigation. *Sci. Rep.* **2023**, *13*, 5213. [[CrossRef](#)] [[PubMed](#)]
81. Zeng, L.; Zhang, S.; Xie, T.; Zhao, C. Contour recognition method of Hall-effect-based whisker sensor. *Meas. Sci. Technol.* **2022**, *33*, 065104. [[CrossRef](#)]
82. Zhang, Y.; Yan, S.; Wei, Z.; Chen, X.; Fukuda, T.; Shi, Q. A small-scale, rat-inspired whisker sensor for the perception of a biomimetic robot: Design, fabrication, modeling, and experimental characterization. *IEEE Robot. Autom. Mag.* **2022**, *29*, 115–126. [[CrossRef](#)]
83. Ahmad Ridzuan, N.A.; Miki, N. Tooth-inspired tactile sensor for detection of multidirectional force. *Micromachines* **2018**, *10*, 18. [[CrossRef](#)]
84. Xie, R.; Zhu, J.; Wu, H.; Zhang, K.; Zou, B.; Zhang, X.; Liang, J.; Zheng, B.; Li, S.; Zhang, W.; et al. 3D-conductive pathway written on leather for highly sensitive and durable electronic whisker. *J. Mater. Chem. C* **2020**, *8*, 9748–9754. [[CrossRef](#)]
85. Lin, C.W.; Zhao, Z.; Kim, J.; Huang, J. Pencil drawn strain gauges and chemiresistors on paper. *Sci. Rep.* **2014**, *4*, 3812. [[CrossRef](#)]
86. Wakabayashi, S.; Yamaguchi, T.; Arie, T.; Akita, S.; Takei, K. Out-of-plane electric whiskers based on nanocarbon strain sensors for multi-directional detection. *Carbon* **2020**, *158*, 698–703. [[CrossRef](#)]
87. Zheng, X.; Kamat, A.M.; Krushynska, A.O.; Cao, M.; Kottapalli, A.G.P. 3D Printed Graphene Piezoresistive Microelectromechanical System Sensors to Explain the Ultrasensitive Wake Tracking of Wavy Seal Whiskers. *Adv. Funct. Mater.* **2022**, *32*, 2207274. [[CrossRef](#)]
88. y Alvarado, P.V.; Subramaniam, V.; Triantafyllou, M. Design of a bio-inspired whisker sensor for underwater applications. In *Proceedings of the SENSORS, 2012 IEEE*, Taipei, Taiwan, 28–31 October 2012; pp. 1–4.

89. Hua, Q.; Liu, H.; Zhao, J.; Peng, D.; Yang, X.; Gu, L.; Pan, C. Bioinspired Electronic Whisker Arrays by Pencil-Drawn Paper for Adaptive Tactile Sensing. *Adv. Electron. Mater.* **2016**, *2*, 1600093. [[CrossRef](#)]
90. Liu, Z.; Qi, D.; Leow, W.R.; Yu, J.; Xiloyannis, M.; Cappello, L.; Liu, Y.; Zhu, B.; Jiang, Y.; Chen, G.; et al. 3D-structured stretchable strain sensors for out-of-plane force detection. *Adv. Mater.* **2018**, *30*, 1707285. [[CrossRef](#)] [[PubMed](#)]
91. Takei, K.; Yu, Z.; Zheng, M.; Ota, H.; Takahashi, T.; Javey, A. Highly sensitive electronic whiskers based on patterned carbon nanotube and silver nanoparticle composite films. *Proc. Natl. Acad. Sci. USA* **2014**, *111*, 1703–1707. [[CrossRef](#)] [[PubMed](#)]
92. Stocking, J.; Eberhardt, W.; Shakhsher, Y.; Calhoun, B.; Paulus, J.; Appleby, M. A capacitance-based whisker-like artificial sensor for fluid motion sensing. In Proceedings of the SENSORS, 2010 IEEE, Waikoloa, HI, USA, 1–4 November 2010; pp. 2224–2229.
93. Assaf, T.; Rossiter, J.; Pearson, M. Contact sensing in a bio-inspired whisker driven by electroactive polymer artificial muscles. In Proceedings of the SENSORS, 2013 IEEE, Baltimore, MD, USA, 3–6 November 2013; pp. 1–4.
94. Droogendijk, H.; Bruinink, C.; Sanders, R.G.; Krijnen, G.J. Non-resonant parametric amplification in biomimetic hair flow sensors: Selective gain and tunable filtering. *Appl. Phys. Lett.* **2011**, *99*, 213503. [[CrossRef](#)]
95. Eberhardt, W.C.; Wakefield, B.F.; Murphy, C.T.; Casey, C.; Shakhsher, Y.; Calhoun, B.H.; Reichmuth, C. Development of an artificial sensor for hydrodynamic detection inspired by a seal's whisker array. *Bioinspir. Biomim.* **2016**, *11*, 056011. [[CrossRef](#)]
96. Delamare, J.; Sanders, R.; Krijnen, G. 3D printed biomimetic whisker-based sensor with co-planar capacitive sensing. In Proceedings of the 2016 IEEE SENSORS, Orlando, FL, USA, 30 October–3 November 2016; pp. 1–3.
97. Fend, M.; Bovet, S.; Hafner, V. The artificial mouse—A robot with whiskers and vision. In Proceedings of the 35th International Symposium on Robotics (ISR 2004), Paris, France, 23–26 March 2004; International Federation of Robotics 2004.
98. Jiang, Y.; Li, J.; Wang, Z.; Qin, Y.; Guo, G.; Zheng, Z.; Bian, Y. Design and fabrication of an E-whisker using a PVDF ring. *Bioinspir. Biomim.* **2021**, *16*, 036007. [[CrossRef](#)]
99. Bebek, O.; Cavusoglu, M.C. Whisker-like position sensor for measuring physiological motion. *IEEE/ASME Trans. Mechatron.* **2008**, *13*, 538–547. [[CrossRef](#)]
100. Kottapalli, A.; Asadnia, M.; Miao, J.; Triantafyllou, M. Harbor seal whisker inspired flow sensors to reduce vortex-induced vibrations. In Proceedings of the 2015 28th IEEE International Conference on Micro Electro Mechanical Systems (MEMS), Estoril, Portugal, 18–22 January 2015; pp. 889–892.
101. Jiang, Y.; Guo, C.; Zhang, Y.; Zhang, W.; Wu, Z.; Shen, H.; Gong, J.; Bian, Y. Design and Fabrication of a Four-Electrodes PVDF Fiber for a Flow Sensor. *IEEE Sens. J.* **2022**, *23*, 1982–1989. [[CrossRef](#)]
102. Ju, F.; Ling, S.F. Sensing fluid viscosity and density through mechanical impedance measurement using a whisker transducer. *Meas. Sci. Technol.* **2013**, *24*, 055105. [[CrossRef](#)]
103. Wang, D.; Li, Y.; Hu, X.; Lu, L.; Xu, P.; Chen, X.; Liu, C.; Wang, L.; Liu, B.; Suo, L.; et al. Electrohydrodynamic jet printed bioinspired piezoelectric hair-like sensor for high-sensitivity air-flow detection. *Smart Mater. Struct.* **2023**, *32*, 095020. [[CrossRef](#)]
104. Wang, X.; Xu, P.; Ma, Z.; Wang, S.; Xie, G.; Xu, M. A bio-inspired whisker sensor based on triboelectric nanogenerators. In Proceedings of the 2020 35th Youth Academic Annual Conference of Chinese Association of Automation (YAC), Zhanjiang, China, 16–18 October 2020; pp. 105–109.
105. Wang, X.; Xu, P.; Liu, J.; Wang, S.; Chen, T.; Guan, T.; Tao, J.; Xu, M. Semi-flexible bionic whisker sensor based on triboelectric nanogenerators. In Proceedings of the 2021 International Conference on Artificial Intelligence and Electromechanical Automation (AIEA), Guangzhou, China, 14–16 May 2021; pp. 194–198.
106. Puneetha, P.; Malle, S.P.R.; Park, S.C.; Kim, S.; Heo, D.H.; Kim, C.M.; Shim, J.; An, S.J.; Lee, D.Y.; Park, K.I. Ultra-flexible graphene/nylon/PDMS coaxial fiber-shaped multifunctional sensor. *Nano Res.* **2023**, *16*, 5541–5547. [[CrossRef](#)]
107. Yu, A.; Chen, L.; Chen, X.; Zhang, A.; Fan, F.; Zhan, Y.; Wang, Z.L. Triboelectric sensor as self-powered signal reader for scanning probe surface topography imaging. *Nanotechnology* **2015**, *26*, 165501. [[CrossRef](#)] [[PubMed](#)]
108. Yu, Z.; Guo, Y.; Su, J.; Huang, Q.; Fukuda, T.; Cao, C.; Shi, Q. Bioinspired, Multifunctional, Active Whisker Sensors for Tactile Sensing of Mobile Robots. *IEEE Robot. Autom. Lett.* **2022**, *7*, 9565–9572. [[CrossRef](#)]
109. Swartz, R.A.; Rajbandari, B.; Winter, B.D. Autonomous Scour Monitoring of Bridges and Embankments Using Bio-Inspired Whisker Flow Sensor Arrays. In Proceedings of the Smart Materials, Adaptive Structures and Intelligent Systems, Newport, RI, USA, 8–10 September 2014; Volume 1
110. Raghunath, G.; Flatau, A.B.; Na, S.-M.; Barkley, B. Development of a Bio-Inspired Tactile Magnetostrictive Whisker Sensor Using Alfenol. In Proceedings of the Smart Materials, Adaptive Structures and Intelligent Systems, Newport, RI, USA, 8–10 September 2014; Volume 2
111. Ju, F.; Ling, S.F. Bioinspired active whisker sensor for robotic vibrissal tactile sensing. *Smart Mater. Struct.* **2014**, *23*, 125003. [[CrossRef](#)]
112. Solomon, J.H.; Hartmann, M.J.Z. Extracting Object Contours with the Sweep of a Robotic Whisker Using Torque Information. *Int. J. Robot. Res.* **2010**, *29*, 1233–1245. [[CrossRef](#)]
113. Reeder, J.T.; Kang, T.; Rains, S.; Voit, W. 3D, reconfigurable, multimodal electronic whiskers via directed air assembly. *Adv. Mater.* **2018**, *30*, 1706733. [[CrossRef](#)]
114. Wang, T.; Kent, T.A.; Bergbreiter, S. Design of Whisker-Inspired Sensors for Multi-Directional Hydrodynamic Sensing. *arXiv* **2023**, arXiv:2307.09569.
115. Sun, X.; Fu, J.H.; Zhao, H.; Xiang, W.; Zhan, F.; Sun, C.; Tang, S.; Wang, L.; Liu, J. Electronic whiskers for velocity sensing based on the liquid metal hysteresis effect. *Soft Matter* **2022**, *18*, 9153–9162. [[CrossRef](#)]

116. Shukla, R.; Routray, P.K.; Subudhi, D.; Manivannan, M. Whiskered Contact-Based Non-Intrusive Vibrometer. In Proceedings of the 2022 10th International Conference on Control, Mechatronics and Automation (ICCMA), Belval, Luxembourg, 9–12 November 2022; pp. 161–167.
117. Wang, R.; Liu, Y.; Bai, B.; Guo, N.; Guo, J.; Wang, X.; Liu, M.; Zhang, G.; Zhang, B.; Xue, C.; et al. Wide-frequency-bandwidth whisker-inspired MEMS vector hydrophone encapsulated with parylene. *J. Phys. D Appl. Phys.* **2016**, *49*, 07LT02. [[CrossRef](#)]
118. Zhang, G.; Ding, J.; Xu, W.; Liu, Y.; Wang, R.; Han, J.; Bai, B.; Xue, C.; Liu, J.; Zhang, W. Design and optimization of stress centralized MEMS vector hydrophone with high sensitivity at low frequency. *Mech. Syst. Signal Process.* **2018**, *104*, 607–618. [[CrossRef](#)]
119. Liu, B.; Herbert, R.; Yeo, W.H.; Hammond, F.L. Kirigami Skin Based Flexible Whisker Sensor. In Proceedings of the 2022 IEEE/RSJ International Conference on Intelligent Robots and Systems (IROS), Kyoto, Japan, 23–27 October 2022; pp. 10015–10020.
120. Rooney, T.; Pearson, M.J.; Pipe, T. Measuring the local viscosity and velocity of fluids using a biomimetic tactile whisker. In Proceedings of the Biomimetic and Biohybrid Systems: 4th International Conference, Living Machines 2015, Barcelona, Spain, 28–31 July 2015; Springer: Berlin/Heidelberg, Germany, 2015; pp. 75–85.
121. Ikedo, A.; Ishida, M.; Kawano, T. Out-of-plane high-density piezoresistive silicon microwire/p-n diode array for force-and temperature-sensitive artificial whisker sensors. *J. Micromech. Microeng.* **2011**, *21*, 035007. [[CrossRef](#)]
122. Nguyen, N.H.; Ho, V.A. Mechanics and Morphological Compensation Strategy for Trimmed Soft Whisker Sensor. *Soft Robot.* **2022**, *9*, 135–153. [[CrossRef](#)]
123. Russell, R.A.; Wijaya, J.A. Recognising and manipulating objects using data from a whisker sensor array. *Robotica* **2005**, *23*, 653–664. [[CrossRef](#)]
124. Pearson, M.J.; Pipe, A.G.; Melhuish, C.; Mitchinson, B.; Prescott, T.J. Whiskerbot: A Robotic Active Touch System Modeled on the Rat Whisker Sensory System. *Adapt. Behav.* **2007**, *15*, 223–240. [[CrossRef](#)]
125. Salman, M.; Pearson, M.J. Whisker-RatSLAM Applied to 6D Object Identification and Spatial Localisation. In *Proceedings of the Biomimetic and Biohybrid Systems*; Springer International Publishing: Cham, Switzerland, 2018; pp. 403–414.
126. Wei, Z.; Shi, Q.; Li, C.; Yan, S.; Jia, G.; Zeng, Z.; Huang, Q.; Fukuda, T. Development of an MEMS based biomimetic whisker sensor for tactile sensing. In Proceedings of the 2019 IEEE International Conference on Cyborg and Bionic Systems (CBS), Munich, Germany, 18–20 September 2019; pp. 222–227.
127. An, J.; Chen, P.; Wang, Z.; Berbille, A.; Pang, H.; Jiang, Y.; Jiang, T.; Wang, Z.L. Biomimetic hairy whiskers for robotic skin tactility. *Adv. Mater.* **2021**, *33*, 2101891. [[CrossRef](#)]
128. Gong, P.; Bhamitipadi Suresh, D.; Jin, Y. Coupling between vortex flow and whisker sensor in cylinder wakes with time-varying streamwise gaps. *Phys. Rev. Fluids* **2023**, *8*, 034701. [[CrossRef](#)]
129. Liu, G.; Jiang, W.; Zheng, X.; Xue, Q. Flow-signal correlation in seal whisker array sensing. *Bioinspir. Biomim.* **2021**, *17*, 016004.
130. Gul, J.Z.; Su, K.Y.; Choi, K.H. Fully 3D Printed Multi-Material Soft Bio-Inspired Whisker Sensor for Underwater-Induced Vortex Detection. *Soft Robot.* **2018**, *5*, 122–132. [[CrossRef](#)]
131. Liu, G.; Jiang, Y.; Wu, P.; Ma, Z.; Chen, H.; Zhang, D. Artificial Whisker Sensor with Undulated Morphology and Self-Spread Piezoresistors for Diverse Flow Analyses. *Soft Robot.* **2023**, *10*, 97–105. [[CrossRef](#)] [[PubMed](#)]

Disclaimer/Publisher’s Note: The statements, opinions and data contained in all publications are solely those of the individual author(s) and contributor(s) and not of MDPI and/or the editor(s). MDPI and/or the editor(s) disclaim responsibility for any injury to people or property resulting from any ideas, methods, instructions or products referred to in the content.